

RESEARCH ARTICLE

Mitochondrial dysfunction in rheumatoid arthritis: A comprehensive analysis by integrating gene expression, protein-protein interactions and gene ontology data

Venugopal Panga^{1,2}, Ashwin Adrian Kallor¹, Arunima Nair¹, Shilpa Harshan^{1,2}, Srivatsan Raghunathan^{1*}

1 Institute of Bioinformatics and Applied Biotechnology (IBAB), Bengaluru, Karnataka, India, **2** Manipal Academy of Higher Education, Manipal, Karnataka, India

* srivatsan@ibab.ac.in



OPEN ACCESS

Citation: Panga V, Kallor AA, Nair A, Harshan S, Raghunathan S (2019) Mitochondrial dysfunction in rheumatoid arthritis: A comprehensive analysis by integrating gene expression, protein-protein interactions and gene ontology data. *PLoS ONE* 14 (11): e0224632. <https://doi.org/10.1371/journal.pone.0224632>

Editor: Dan Mishmar, Ben-Gurion University of the Negev, ISRAEL

Received: May 22, 2019

Accepted: October 17, 2019

Published: November 8, 2019

Peer Review History: PLOS recognizes the benefits of transparency in the peer review process; therefore, we enable the publication of all of the content of peer review and author responses alongside final, published articles. The editorial history of this article is available here: <https://doi.org/10.1371/journal.pone.0224632>

Copyright: © 2019 Panga et al. This is an open access article distributed under the terms of the [Creative Commons Attribution License](https://creativecommons.org/licenses/by/4.0/), which permits unrestricted use, distribution, and reproduction in any medium, provided the original author and source are credited.

Data Availability Statement: All relevant data are within the manuscript and its Supporting Information files.

Abstract

Several studies have reported mitochondrial dysfunction in rheumatoid arthritis (RA). Many nuclear DNA (nDNA) encoded proteins translocate to mitochondria, but their participation in the dysfunction of this cell organelle during RA is quite unclear. In this study, we have carried out an integrative analysis of gene expression, protein-protein interactions (PPI) and gene ontology data. The analysis has identified potential implications of the nDNA encoded proteins in RA mitochondrial dysfunction. Firstly, by analysing six synovial microarray datasets of RA patients and healthy controls obtained from the gene expression omnibus (GEO) database, we found differentially expressed nDNA genes that encode mitochondrial proteins. We uncovered some of the roles of these genes in RA mitochondrial dysfunction using literature search and gene ontology analysis. Secondly, by employing gene co-expression from microarrays and collating reliable PPI from seven databases, we created the first mitochondrial PPI network that is specific to the RA synovial joint tissue. Further, we identified hubs of this network, and moreover, by integrating gene expression and network analysis, we found differentially expressed neighbours of the hub proteins. The results demonstrate that nDNA encoded proteins are (i) crucial for the elevation of mitochondrial reactive oxygen species (ROS) and (ii) involved in membrane potential, transport processes, metabolism and intrinsic apoptosis during RA. Additionally, we proposed a model relating to mitochondrial dysfunction and inflammation in the disease. Our analysis presents a novel perspective on the roles of nDNA encoded proteins in mitochondrial dysfunction, especially in apoptosis, oxidative stress-related processes and their relation to inflammation in RA. These findings provide a plethora of information for further research.

Funding: We thank the department of Information Technology, Biotechnology and Science & Technology (IT, BT and S&T), Government of Karnataka, India for infrastructure support. VP received fellowships from the Institute of Bioinformatics and Applied Biotechnology (IBAB) as well as from the Council of Scientific and Industrial Research (CSIR), Government of India (Gol) (File No. 09/1086(0001)/2012-EMR-1), URL: <http://www.csirhrdg.res.in/>. SR is a faculty at IBAB. This project was partially supported by a grant from the Department of Biotechnology, Gol (BTPR12422/MED/31/287/2014, URL: <http://www.dbtindia.nic.in/>). The funders had no role in study design, data collection and analysis, decision to publish, or preparation of the manuscript.

Competing interests: The authors have declared that no competing interests exist.

Introduction

Mitochondrial dysfunction prevails among numerous diseases, including RA, Sjögren's syndrome, neurodegenerative diseases, diabetes, cancer and obesity [1–5]. Genomic technologies and computational approaches played a vital role in our understanding of mitochondrial dysfunction in several diseases like Leigh syndrome, cardiovascular diseases, obesity and infantile-onset mitochondrial encephalopathy [6–12]. These approaches have also discerned the mechanics of calcium uniporter in mitochondrial biology and associated diseases [7, 13–15]. Further, investigations into metabolic profiling and whole-exome sequencing data point to metabolic abnormalities concerned with mitochondria and biallelic mutations leading to instability in mitoribosomal subunits in Leigh syndrome [6, 8].

Mitochondria, which are membrane-bound cell organelles, are the primary generators of adenosine triphosphate (ATP). The respiratory chain complexes, which are part of the mitochondrial oxidative phosphorylation (OxPhos), are necessary for the production of ATP. The genome of this organelle has 13 protein-coding genes, which are associated with the OxPhos pathway. It is understood that 1158 nDNA encoded proteins get translocated to this cell organelle [16], and some of them are crucial for the OxPhos pathway. However, the functional roles of many of these proteins in RA mitochondrial dysfunction are uncertain, creating a serious lacuna in our understanding of this disease. An integrative analysis of these proteins using gene expression, PPI, gene ontology and network theory offers an excellent opportunity for deducing some of their roles.

About 1% of the world's population is affected by RA [17]. It is a chronic inflammatory disease that usually affects the small synovial joints of the hands and feet. The disease synovium gets inflamed (a condition called synovitis) and invades articular cartilage and bone, forming a layer of granulation tissue called pannus. Further, synovitis causes irreversible damage to the synovium in joints [18]. Moreover, the cells of the RA synovium (synoviocytes) secrete inflammatory cytokines and articular cartilage-degrading enzymes, such as matrix metalloproteinases (MMPs), which further aggravate the disease.

The composition of cell types in a healthy synovium is different to that of RA. The healthy synovium primarily contains two cell types, macrophage-like synoviocytes (MLS) and fibroblast-like synoviocytes (FLS) [19]. Other cell types such as leucocytes can be seen in small numbers [19]. In contrast, the RA synovium is expanded and forms pannus and contains resident MLS and FLS as well as heavily infiltrated leucocytes [20–21].

The pannus in RA, like a tumour, increases demand for energy (ATP) in the synovium. Additionally, the dysregulated synovial microvasculature results in a poor supply of oxygen to the tissue, causing hypoxia. Both the increased energy demand on mitochondrial electron transport and hypoxia could lead to an enhanced production of ROS, creating oxidative stress in synoviocytes [1]. Further, an inverse correlation between synovitis and the partial pressure of oxygen in the synovium testifies to the role of hypoxia in arthritis [22]. Moreover, hypoxia might induce proinflammatory pathways, through hypoxia-inducible factor-1 α (HIF-1 α), nuclear factor κ B (NF- κ B), Janus kinase-signal transducer and activator of transcription (JAK-STAT), activator protein 1 (AP-1) and Notch. Most notably, anti-tumour necrosis factor therapy has significantly decreased synovial hypoxia in vivo, indicating that it is a crucial event in arthritis [1, 22–25]. This elucidates that hypoxia and ROS are relevant to RA mitochondrial dysfunction.

Superoxide anion (O₂⁻), hydrogen peroxide (H₂O₂) and hydroxyl radical (\cdot OH) are collectively called ROS [26–27]. The components of ROS can damage DNA, proteins, lipids and many other molecules. Synovial fluid (SF) and plasma samples as well as blood lymphocytes and polymorphonuclear leucocytes from RA patients have significantly higher mitochondrial

DNA (mtDNA) and oxidatively damaged DNA adduct, 8-hydroxyl-2'-deoxyguanosine (8-oxodG), than non-arthritic samples. Further, both the mtDNA and 8-oxodG levels in SF correlate with the presence of rheumatoid factor in RA patients [28–29]. This underlines the existence of ROS-mediated damage of mitochondria in this disease. Other oxidative stress markers, such as protein carbonyls are significantly higher in the serum of RA patients compared to healthy controls. Treatment of these patients with infliximab resulted in a significant decrease of the carbonyls [30]. Iron, a catalyst for the formation of $\cdot\text{OH}$ from H_2O_2 via the Fenton's reaction, is present in the diseased synovium [31]. Oxidised low-density lipoproteins and lipid peroxidation as well as the latter's correlation with the concentration of Iron ions were observed in SF of RA patients [32–33]. Furthermore, hyaluronate-derived small oligosaccharides are present in the inflamed disease joints, revealing the activity of ROS [34]. The ROS-mediated damage of mitochondria might also result in angiogenesis and cartilage destruction, the latter of which ensues through the up-regulation of MMPs [1, 25, 35–36]. Besides, there is an inverse association between the dietary intake of antioxidants and the prevalence of RA as well as the levels of antioxidants and the disease inflammation [37–42]. Moreover, an element of ROS, $\text{O}_2^{\cdot-}$ reacts with nitric oxide (NO) to form peroxynitrite (ONOO^-), which is a component of the reactive nitrogen species (RNS). This reactive species plays a role in the NF- κ B-mediated production of inflammatory mediators, such as tumour necrosis factor (TNF), interleukin-1 beta (IL-1 β) and inducible nitric oxide synthase (iNOS) [43].

To summarise, the pannus increases ATP demand and the dysregulated microvasculature creates hypoxia. Both the conditions can generate ROS in RA synovial mitochondria and the immediate targets of these free radicals are mtDNA, proteins and lipids. Supporting this phenomenon in RA, elevated levels of the damaged mtDNA, proteins and lipids were observed in SF, plasma and leucocytes of the patients. Additionally, both the hypoxia and ROS are known to induce pro-inflammatory HIF-1 α , NF- κ B, JAK-STAT, AP-1 and Notch pathways. As stated earlier, 1158 nDNA encoded proteins get translocated to mitochondria and several of them could be involved in the pathways concerned with the generation of ROS. So, it is of great pathophysiological relevance to elucidate the roles of these proteins in mitochondrial dysfunction and their connection to ROS-mediated damage, hypoxia, ATP synthesis and inflammation in RA.

In RA, apoptosis is required to control synovial hyperplasia. Apoptosis can occur by two different pathways, the extrinsic and the intrinsic, of which the latter could be initiated in mitochondria in response to oxidative stress. Both the pathways culminate in the activation of a cascade of proteases, called caspases. It has been shown that the extrinsic pathway is inactive in RA FLS [44]. Fas, which is a pro-apoptotic molecule and known to be involved in the extrinsic pathway, has been found to induce inflammation rather than apoptosis in RA FLS. However, this process depends on caspase-8 (CASP8) activity and FLICE-like inhibitory protein (FLIP) expression [45]. Therefore, studying the intrinsic pathway might give clues on the regulation of synovial hyperplasia. Hence it is important to understand the roles of the nDNA encoded proteins that could be implicated in this pathway.

In the current study, we followed an integrated approach that uses microarray data, PPI, gene ontology and network analysis. Six microarray gene expression datasets related to RA and healthy synovium were obtained from GEO, and they were analysed to discover differentially expressed genes (DEGs) encoding mitochondrial proteins. Further, a mitochondrion-specific PPI network has been created based on the information from seven publicly available databases. We also performed gene ontology analysis (GO) using the Search Tool for the Retrieval of Interacting Genes (STRING) database for identifying significantly enriched biological processes (BP), molecular functions (MF) and cellular components (CC). In addition to a discussion on the roles of nDNA encoded proteins in RA mitochondrial dysfunction based

on available information in the literature, a model for the relation between mitochondrial dysfunction and the disease inflammation has also been framed.

Methods

Data collection

The mRNA expression datasets (GSE77298, GSE7307, GSE12021, GSE55235 and GSE55457) were retrieved from GEO, which is a public National Center for Biotechnology Information (NCBI) database. [Table 1](#) gives a detailed account of the mRNA expression datasets. All the datasets were downloaded in raw data file format for analysis.

Construction of mitochondrial PPI network in RA synovium

The mitochondrial PPI network in RA synovium was created by pooling the experimentally determined interactions in human cells. They were obtained from seven publicly available resources, namely the biological general repository for interaction datasets (BioGRID), IntAct, the molecular interaction (MINT), STRING, the human protein reference database (HPRD), the database of interacting proteins (DIP) and CRG [46–52]. Among them, the first four databases have confidence scores for each interaction. The higher the score the more is the confidence for the interaction to occur. For the current study, from each of these four, we have got more reliable interactions by putting a cut-off to the confidence scores. The cut-off was decided in such a way that the interactions having a confidence score more than the median of the score distributions were selected. From DIP, the interactions with the core quality status were considered. From HPRD and CRG, which do not have confidence scores, only those interactions which have at least two publication evidences were considered. Collectively, a total of 387,242 interactions were obtained from all the seven resources. Then, to create the mitochondrial PPI network, only the interactions of those proteins that get localised to mitochondria were chosen using MitoCarta [16], which is a compendium of 1158 nDNA genes that encode mitochondrial proteins.

Furthermore, to make this interactome specific to the synovial tissue, we measured the co-expression of the interacting partners of these interactions using the gene expression data from six microarray datasets. [Table 1](#) gives detailed information about these datasets. For each dataset, the raw intensities were normalised using the RMA algorithm. For the interacting partners of each interaction, we computed the Pearson correlation coefficient of the normalised expression values across all disease samples. Only those interactions with a Pearson correlation coefficient > 0.7 between the partners, in at least one microarray dataset, were considered co-expressed in the synovial tissues. The resulting interactions were used to create the undirected mitochondrial PPI network, using the ‘igraph’ package in R. The hubs of this network were identified using the same package in R.

Table 1. Details of microarray datasets used in this study.

S.No.	GEO Accession	PubMed ID	Microarray Platform	Probe Number	Number of Samples	
					RA	Control
1	GSE77298	26711533	Affymetrix Human Genome U133 Plus 2.0 Array	54675	16	7
2	GSE7307	-	Affymetrix Human Genome U133 Plus 2.0 Array	54675	5	9
3	GSE12021	18721452	Affymetrix Human Genome U133A Array	22283	12	9
4	GSE12021	18721452	Affymetrix Human Genome U133B Array	22645	12	4
5	GSE55457	24690414	Affymetrix Human Genome U133A Array	22283	13	10
6	GSE55235	24690414	Affymetrix Human Genome U133A Array	22283	10	10

<https://doi.org/10.1371/journal.pone.0224632.t001>

Differential expression analysis of microarray data

The microarray experiments, considered in this study, were carried out on RA and normal synovial tissues by other workers (Table 1). The RA samples used in these studies were obtained by tissue excision upon joint replacement/synovectomy surgery from RA patients. Similarly, the control samples were obtained from either postmortem or traumatic joint injury cases. In four of the six datasets (GSE12021 (HGU133A), GSE12021 (HGU133B), GSE55235 and GSE55457), for which the information on duration and severity of the disease is available, the duration of the disease in the patients was reported to be a mean of at least 12 years. The number of American rheumatism association (ARA) (now, American college of Rheumatology) criteria for RA was reported to be a mean of at least five [53–54]. The patients, who participated in five of the six studies, are from the Netherlands and Germany. For one study (GSE7307), the demography of patients is not available.

We re-analysed all the datasets using the R/Bioconductor statistical package. The intensities were normalised using two algorithms, MAS5 and RMA, separately. The differential expression of the genes between RA and control groups was computed using the two sample independent t-test. A p-value < 0.05 and a fold-change of > 1.5 in the up or down direction were taken as the cut-off values for differential expression. Further, the following conditions were imposed for deciding a differentially expressed gene across the datasets:

1. For one dataset, if the gene is selected by both the normalisation methods in the same direction (up or down)
2. For multiple datasets, if the gene is selected by both the normalisation methods in at least one dataset or by complementary normalisation methods in at least two datasets.
3. If the gene is up-regulated in at least one dataset and not down-regulated in any of the remaining, we call it a consistently up-regulated gene. A similar criterion was applied for a down-regulated gene. On the other hand, if a gene shows up-regulation in some and down-regulation in the other datasets, we call it a mixed-regulated gene.

Since we are particularly interested in nuclear genes that encode mitochondrial proteins, and in order to maximise the DEGs of mitochondrial proteins, we did not correct the p-value. However, for most of the analyses performed, the genes that were selected in at least two or three datasets were considered. Further, the DEGs were used for integrative analysis and hence the false positives might be reduced.

Gene ontology and pathway enrichment analysis

The GO and pathway enrichment analyses were carried out using the STRING database. These analyses identify enriched GO terms and KEGG (Kyoto Encyclopedia of Genes and Genomes) pathways for a given list of genes by employing a hypergeometric test that was discussed elsewhere [55–56]. A false discovery rate (FDR) < 0.01 was considered as the cut-off for the significantly enriched GO terms and pathways.

Results

Creation of mitochondrial PPI network in the RA synovium

High-confident PPI from seven public resources, namely BioGRID, IntAct, MINT, STRING, HPRD, DIP and CRG, were used to construct this network [46–52]. The first four databases provide a confidence score, which is a measure of reliability, for each interaction. From each of these databases, only the interactions with the scores above the median of the confidence score

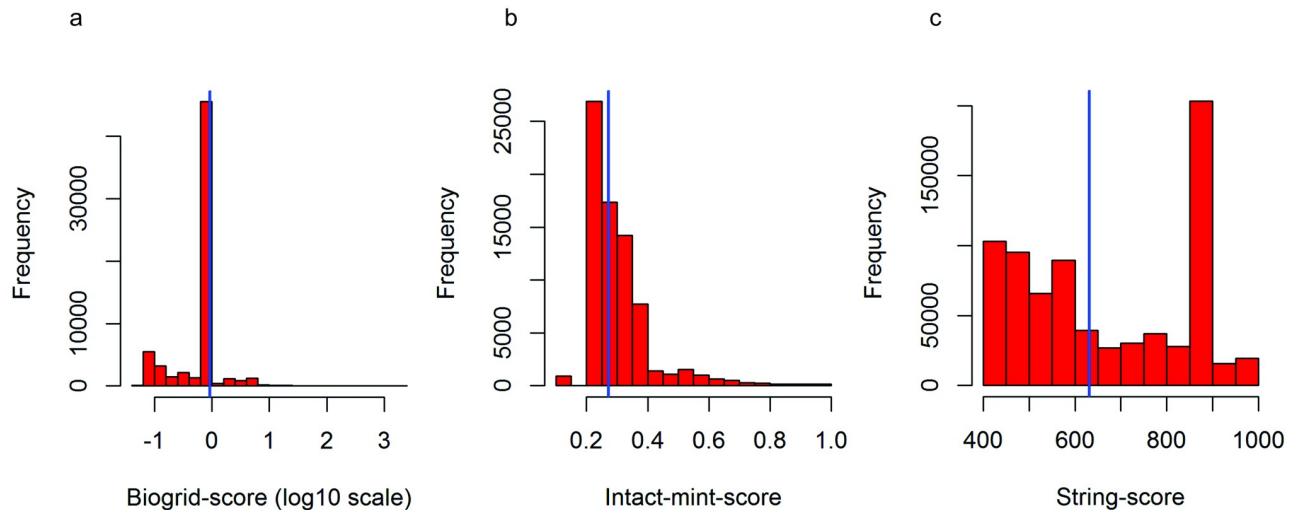


Fig 1. Confidence score distributions of PPI in (a) Biogrid, (b) Intact and Mint, and (c) String. The blue vertical line in all of them corresponds to the median of the distributions. The interactions which have a confidence score above the median were considered for the current study.

<https://doi.org/10.1371/journal.pone.0224632.g001>

distributions were extracted (Fig 1). From DIP, only those interactions which have core quality status (a reliability parameter specific to DIP) were extracted. From HPRD and CRG, the interactions with at least two publication evidences were selected. This resulted in 387,242 reliable interactions which constitute ~40% of the total interactions in these databases. Then, we applied a filter requiring both the interacting partners to be nDNA encoded mitochondrial proteins, the list of which could be found in MitoCarta [16]. This has returned an interactome with 7023 interactions, representing 926 of the 1158 MitoCarta genes (79.96%). In order to make the interactome specific to the RA synovium, we computed the co-expressions between the interacting partners using RA synovial microarray data (Table 1). For each pair of interacting proteins, their expression levels across the RA disease samples in a given microarray dataset were used to compute the Pearson's correlation coefficient (ρ) as a measure of co-expression. The interacting partners with a $\rho > 0.7$ between their gene expression values in at least one of the six microarray datasets were considered to be co-expressed in the synovium. This selection criterion, which was chosen to maximise the number of PPI with the co-expressed interacting partners, resulted in an interactome with 2708 interactions and 665 genes, representing 57.42% of MitoCarta genes. In this interactome, on an average, each protein is connected to four other proteins. None of the interacting partners were co-expressed in all the six datasets. Of the 2708 interactions, 13 have the co-expressed interacting partners in five microarray datasets; 65 in four; 184 in three; 618 in two and 1828 in one datasets. With these interactions, we have created the mitochondrial PPI network using the 'igraph' package in R. In order to identify the localisation of the network proteins in mitochondria, a GO analysis for the cellular component (CC) term was performed using the STRING database [55–56]. It was observed that the majority of the network proteins get translocated to the mitochondrial inner membrane and matrix (S1 Fig).

Differential expression of nuclear genes encoding mitochondrial proteins

Differential expression analysis between RA and healthy human synovial tissue samples was carried out using the six microarray datasets obtained from GEO (Table 1). The requirement for differential expression in a dataset was set to be a fold-change > 1.5 (up or down

regulation) and a p-value < 0.05. Of the 665 PPI network genes, 131 were found to be differentially expressed in at least one RA synovial microarray dataset (S1 Table). The criterion of a gene having a differential expression in at least one of the six datasets was decided so as to maximise the selection of mitochondrial DEGs. The whole network indicating the up and down DEGs, which can be visualised using the Cytoscape tool, is in S1 File. The 131 genes include 46 consistently up-, 73 consistently down- and 12 mixed-regulated genes (for methodological details, see ‘Methods’ section). Another 77 of the MitoCarta members, which are not part of the network, were also differentially expressed in at least one dataset (S2 Table). Thus, it makes a total of 208 mitochondrial DEGs (83 up-, 111 down- and 14 mixed-regulated). Their differential expression across the six studies is as follows; only one of the 208 genes was a DEG in all the six studies; three (1.44%) genes in five studies; four (1.92%) in four; 15 (7.21%) in three; 60 (28.84%) in two and 125 (60.09%) in one study.

Mitochondrial DEGs that were found in at least three datasets are in Table 2 (13 up-, 6 down- and 4 mixed-regulated). Among them, the following up-regulated genes are highlighted in respect of their functions in mitochondria. Acyl-CoA thioesterase 7 (ACOT7) is an enzyme that hydrolyses long-chain fatty acids such as palmitoyl-CoA. Kynurenine 3-monooxygenase (KMO) is an enzyme that catalyses the hydroxylation of kynurenine to form 3-hydroxykynurenine. This enzyme has been reported to be involved in the generation of oxidative radicals as well as in cytokine-mediated inflammation [57]. Leucine amino peptidase 3 (LAP3) is involved

Table 2. The differentially expressed genes (DEGs) of mitochondrial proteins in at least three synovial microarray datasets.

S.No.	Gene	Number of RA synovial datasets in which the gene was differentially expressed			Type of regulation	Max fold-change	
		Up-regulated	Down-regulated	Total		Linear	log base 2
1	AK4	1	2	3	Mixed	1.87	0.90
2	AKR1B10	0	3	3	Down	0.26	-1.94
3	BCL2	3	1	4	Mixed	0.38	-1.39
4	C10orf10	1	2	3	Mixed	0.17	-2.55
5	DNAJC15	3	0	3	Up	1.72	0.78
6	IDH2	3	0	3	Up	3.66	1.87
7	MAOA	0	3	3	Down	0.09	-3.47
8	MCCC1	0	3	3	Down	0.58	-0.78
9	PDK4	0	3	3	Down	0.12	-3.05
10	YME1L1	3	0	3	Up	3.22	1.68
11	PRDX4	3	0	3	Up	4.62	2.20
12	UCP2	4	0	4	Up	7.94	2.98
13	C10orf2	0	3	3	Down	0.61	-0.71
14	ACOT7	5	0	5	Up	2.75	1.45
15	EFHD1	0	3	3	Down	0.26	-1.94
16	IFI27	4	0	4	Up	3.54	1.82
17	KMO	5	0	5	Up	4.55	2.18
18	PLGRKT	3	0	3	Up	2.59	1.37
19	SLC16A7	2	4	6	Mixed	0.28	-1.83
20	CASP8	3	0	3	Up	2.4	1.26
21	LAP3	5	0	5	Up	2.73	1.44
22	PDK1	4	0	4	Up	4.81	2.26
23	C15orf48	3	0	3	Up	30.45	4.92

The number of datasets in which the gene was up/down-regulated is also given in the table along with the maximum observed fold-change of the genes among the datasets.

<https://doi.org/10.1371/journal.pone.0224632.t002>

in the degradation of glutathione, a scavenger of free radicals [58], indicating the likely impairment in the detoxification of ROS. Pyruvate dehydrogenase kinase 1 (PDK1) inhibits pyruvate dehydrogenase activity and is known to play an integral role against hypoxia- and oxidative stress-mediated apoptosis [59]. Interferon alpha inducible protein 27 (IFI27) is known to be involved in cytokine signalling and apoptosis. Interestingly, this protein activates an apoptotic caspase, CASP8, which was also up-regulated in the microarray data [60]. Uncoupling protein 2 (UCP2) is implicated in the transfer of anions from the inner to the outer membrane and protons from the outer to the inner membrane, and it is known to control ROS [61]. Peroxiredoxin-4 (PRDX4) is an antioxidant enzyme which detoxifies H₂O₂ and regulates NF- κ B activation [62]. Nonetheless, because of its high reactivity, this enzyme is susceptible to overoxidation and inactivation by H₂O₂ [63]. YME1 like 1 ATPase (YME1L1), which is an ATP-dependent metalloprotease, is known to function in the maintenance of mitochondrial morphology and accumulation of respiratory chain subunits [64–65]. Isocitrate dehydrogenase 2 (IDH2) is implicated in the production of NADPH and in the protection of cells from ROS. DnaJ heat shock protein family (Hsp40) member C15 (DNAJC15) negatively regulates respiratory chain and generation of ATP.

Similarly, the six genes that were down-regulated in at least three datasets participate in the following functions. MCCC1 encodes α subunit of 3-methylcrotonoyl-CoA carboxylase (3-MCC), which is an enzyme that is involved in the breakdown of leucine. Monoamine oxidase A (MAOA) catalyses the oxidative deamination of amines, such as serotonin, norepinephrine and dopamine, and its deficiency is known to induce aggression [66–67]. The transcription factors, specificity protein 1 (SP1), GATA binding protein 2 (GATA2) and TATA box binding protein (TBP) regulate the expression of this gene [68]. EF-hand domain-containing protein 1 (EFHD1) is a calcium ion sensor. Some of the other down-regulated genes are AKR1B10, PDK4 and C10orf2.

The mixed-regulated gene, solute carrier family 16 member 7 (SLC16A7) is involved in the transport of metabolites such as monocarboxylates and pyruvate. Similarly, adenylate kinase 4 (AK4) is implicated in the metabolism of nucleotides.

The largest genome-wide association study meta-analysis of RA cases and controls has identified 98 disease risk genes [69]. Six of them, C1QBP, SUOX, ACSL6, UNG, CYP27B1 and CASP8 are MitoCarta genes. Among these, only CASP8 was a DEG, and C1QBP and CYP27B1 are part of the created mitochondrial network. The role of these genes in RA and their involvement in mitochondrial dysfunction remain to be ascertained.

Effects of medical therapies on gene expression

Of the six open-source microarray datasets we analysed, RA patients in one (GSE7307) were not treated with therapies, while the patients belonging to three others (GSE12021 (HGU133A), GSE12021 (HGU133B) and GSE55457) underwent different combinations of medical therapies. The information on medications is not available for two datasets (GSE55235 and GSE77298). All the details of medical therapies available for the datasets are listed in [Table 3](#).

It is seen within a dataset that some patients have received the same combination of medical therapies whereas others received different combinations. To test if the gene expressions are influenced by these medical therapies, the samples in each microarray dataset were hierarchically clustered based on the mRNA levels of the DEGs that were differentially expressed in at least three microarray datasets ([Table 2](#)). The cluster results are shown as heatmaps with dendrograms ([S2–S7 Figs](#)). In GSE7307, GSE55235 and GSE55457, RA and control samples were clustered into separate groups ([S2–S4 Figs](#)). In GSE12021 (HGU133A) and GSE12021

Table 3. Medical therapies initiated on RA patients that participated in the microarray studies.

Dataset	Patients	Medical Therapies
GSE7307		All the patients were not treated
GSE12021A	RA1	NSARD + Azulfidine + Prednisolone
	RA2	NSARD + MTX + Prednisolone
	RA3	NSARD + MTX+ Prednisolone
	RA4	NSARD + Azulfidine + Prednisolone + MTX
	RA5	NSARD + MTX + Prednisolone
	RA6	NSARD + Azulfidine + Prednisolone
	RA7	MTX + Prednisolone
	RA8	NSARD
	RA9	NSARD + Prednisolone
	RA10	NSARD + Prednisolone
	RA11	COX-2 inhibitor + Prednisolone + Quensyl
	RA12	NSAID + Tilidin + Prednisolone
GSE12021B	RA1	NSARD + Azulfidine + Prednisolone
	RA2	NSARD + MTX + Prednisolone
	RA3	NSARD + MTX+ Prednisolone
	RA4	NSARD + Azulfidine + Prednisolone + MTX
	RA5	NSARD + MTX + Prednisolone
	RA6	NSARD + Azulfidine + Prednisolone
	RA7	MTX + Prednisolone
	RA8	NSARD
	RA9	NSARD + Prednisolone
	RA10	NSARD + Prednisolone
	RA11	COX-2 inhibitor + Prednisolone + Quensyl
	RA12	NSAID + Tilidin + Prednisolone
GSE55457	RA1	NSARD + Azulfidine + Prednisolone
	RA2	NSARD + MTX + Prednisolone
	RA3	NSARD + MTX+ Prednisolone
	RA4	NSARD + Azulfidine + Prednisolone + MTX
	RA5	NSARD + MTX + Prednisolone
	RA6	NSARD + Azulfidine + Prednisolone
	RA7	MTX + Prednisolone
	RA8	NSARD
	RA9	NSARD + Prednisolone
	RA10	no therapy used
	RA11	NSARD + Prednisolone
	RA12	COX-2 inhibitor + Prednisolone + Quensyl
	RA13	NSAID + Tilidin + Prednisolone
GSE55235		Therapies not mentioned for these two datasets
GSE77298		

NSARD, nonsteroidal anti-rheumatic drug; MTX, methotrexate; COX-2, cyclooxygenase-2; NSAID, nonsteroidal anti-inflammatory drug

<https://doi.org/10.1371/journal.pone.0224632.t003>

(HGU133B), some RA samples were clustered into a separate group while others were clustered with control samples (S5 and S6 Figs), showing that there is a drug effect. In GSE77298, some RA samples were clustered with healthy controls but drug therapies are not available for this dataset (S7 Fig).

In order to find the effect of medical therapies on the differential expression of genes, we removed the RA samples that were clustered with healthy controls from GSE12021 (HGU133A) and GSE12021 (HGU133B) datasets and repeated the differential expression analysis for the 23 genes listed in Table 2. Surprisingly, with the same selection criteria of differential expression, all the 23 genes were retained. The heatmaps of the expression levels of the genes in these two datasets after eliminating the RA samples that clustered with healthy controls are shown in S8 and S9 Figs. We notice the complete separation of controls from RA samples in the clusters.

From the above analysis, we find that the 23 genes were differentially expressed in at least three datasets in both of the following cases.

Case 1: all RA and control samples in all the six studies

Case 2: all RA samples except those that clustered with healthy controls in GSE12021 (HGU133A) and GSE12021 (HGU133B) and all controls in all the six studies. Since the 23 genes were differentially expressed in at least three datasets in both the cases, we conclude that these genes were not affected by the therapy initiation.

In addition to the above analysis, we analysed two other microarray datasets (GSE77344 and GSE11237) where patients with diseases unrelated to RA were treated with prednisone or celecoxib. Prednisone is the prodrug form of prednisolone, while celecoxib is a COX-2 inhibitor. Prednisolone and COX-2 inhibitors are part of the therapies received by RA patients shown in Table 3. In the dataset GSE77344 [70], whole blood was collected from patients with chronic obstructive pulmonary disease who were either treated ($n = 31$) or not treated ($n = 103$) with prednisone. GSE11237 [71] contained colorectal primary adenocarcinomas surgically removed from 23 patients, 11 of whom received 400 mg celecoxib two times per day for seven days prior to surgery and 12 who did not receive the treatment. In addition to this, we also analysed GSE45867 [72] which had paired synovial tissue biopsies from 8 early RA patients naive to methotrexate or DMARDs. The samples were collected before and 12 weeks after the initiation of methotrexate therapy. Hierarchical clustering of the samples based on the expression levels of the 23 genes normalized across samples did not show any separation of treated and nontreated samples, or pre and post treatment samples (S10–S12 Figs). Differential expression analysis with the criteria used for the RA datasets (fold change $> |1.5|$ and p value ≤ 0.05) revealed one gene out of the 23 was upregulated in GSE77344 (MAOA, fold change = 3.9, p value = 0.001), while no differential regulation was found for any of the 23 genes in GSE11237 and GSE45867. Thus we believe that the effects of these specific treatments on the candidate genes are negligible, and the differential regulation observed in the RA datasets is more likely due to the disease itself.

Identification of hubs of the PPI network

To further elucidate the properties of the mitochondrial PPI network, we performed network analysis. For each node, we chose to measure the network parameter ‘degree’ which is the number of edges a node can have. The probability distribution of the degree of nodes in the created mitochondrial PPI network along with power-law fit to the data is shown in Fig 2. The degree distribution of the network follows a power law $P(k) \sim k^{-\alpha}$ (with the degree coefficient, $\alpha = 1.82$), which is a property of scale-free networks [73]. From this network, we identify a small number of important nodes, called hubs, which are directly connected to a large number of interacting partners. Analogous to social networks, the hub proteins with a higher number of neighbours are crucial to PPI networks as their removal causes dysfunction of the system.

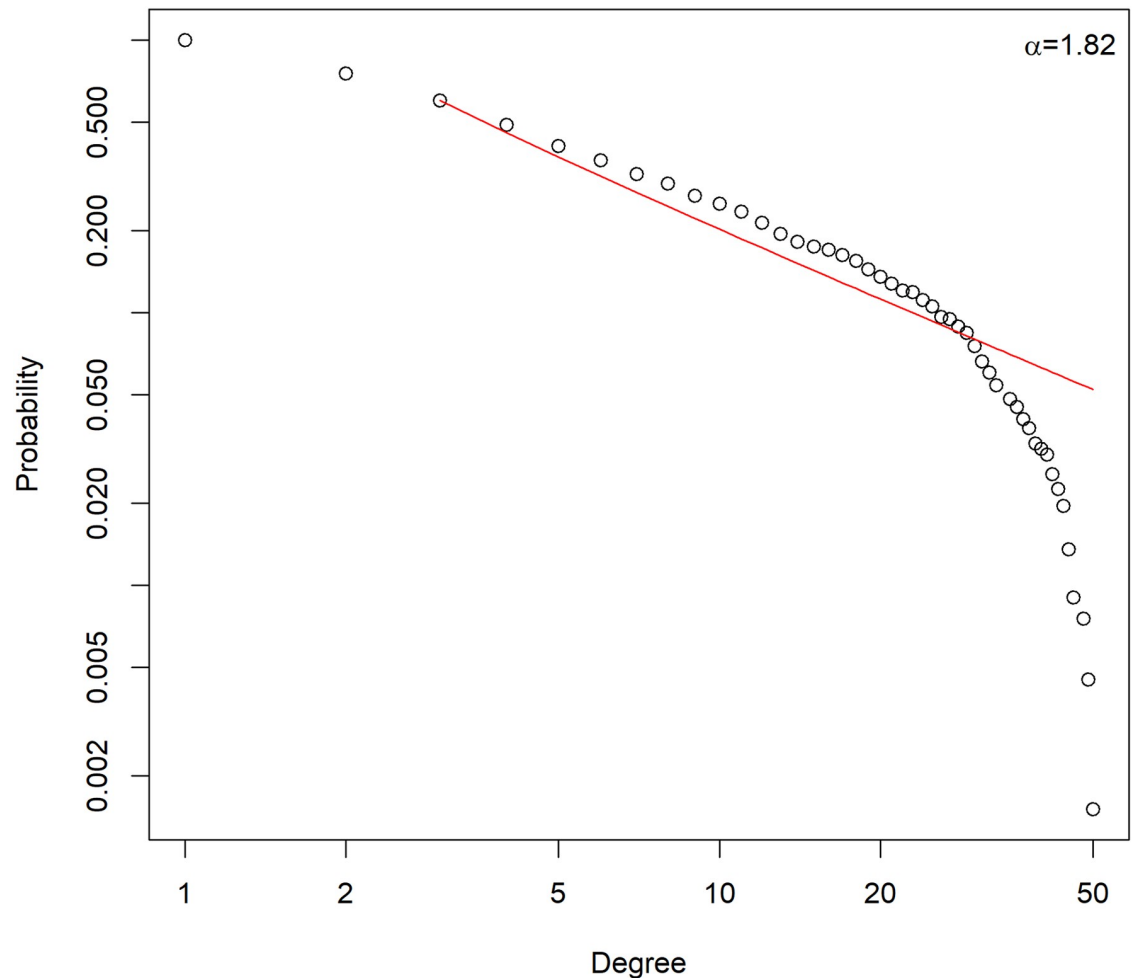


Fig 2. Degree distribution of the mitochondrial PPI network (nodes: 665, edges: 2708), following a power law. The circles represent the fraction of nodes with a given degree and the solid line indicates the power-law fit to the data.

<https://doi.org/10.1371/journal.pone.0224632.g002>

The immediate neighbours of all the 665 proteins in the mitochondrial PPI network were determined. The top 50 proteins in the decreasing order of the number of their immediate neighbours are listed in [Table 4](#). The entire list of all the network proteins and the number of their immediate neighbours—including the extent of DEGs among them—could be found in [S3 Table](#). The distributions of the proteins in terms of the total number of neighbours and the proportion of DEGs among them are shown in [S13 Fig](#).

Each of the network proteins has at least one neighbour. Among them, 167 have at least 10 neighbours. Most of the network proteins are connected to one or a few DEGs. The scatter plot between the number of neighbours and the number of DEGs among the neighbours for individual proteins is shown in [Fig 3](#). It would be interesting to look at the hubs with a high number of neighbours containing higher number of DEGs among them. For example, the upper right-side rectangle of the figure has the hubs connected to at least 27 neighbours having a minimum of seven DEGs among them. The hubs which have fallen into this rectangle are given in [Table 5](#). They could be considered crucial for mitochondrial functions in the RA diseased synovium because of a high number of DEGs among the neighbours.

Table 4. Number of neighbours for the top 50 mitochondrial PPI network hub proteins.

S.No.	Protein	Neighbours	DEGs	Up DEG	Down DEG	mixed DEGs
1	UQCR10	50	9	2	6	1
2	MRPL4	49	4	0	4	0
3	NDUFV2	49	8	0	7	1
4	UQCRC2	48	6	0	5	1
5	UQCRQ	48	9	3	5	1
6	NDUFS3	46	5	1	4	0
7	MRPL47	45	4	0	4	0
8	NDUFA13	45	8	2	5	1
9	NDUFB8	45	7	2	4	1
10	ATP5O	44	8	2	5	1
11	MRPL24	44	3	0	3	0
12	NDUFS6	44	11	4	6	1
13	UQCRC1	44	7	2	4	1
14	CYC1	43	6	2	4	0
15	NDUFAB1	43	8	1	6	1
16	MRPL13	42	5	0	5	0
17	MRPL16	42	2	0	2	0
18	ATP5C1	41	7	1	5	1
19	MRPS16	41	2	2	0	0
20	NDUFB10	41	7	1	5	1
21	NDUFA9	40	7	2	4	1
22	MRPL15	39	6	0	6	0
23	COX5B	38	7	2	4	1
24	NDUFA8	38	4	0	3	1
25	UQCRC1	38	5	2	3	0
26	COX6A1	37	2	0	2	0
27	NDUFA2	37	7	2	5	0
28	MRPL3	36	5	0	5	0
29	NDUFB9	36	4	2	2	0
30	SDHB	36	5	0	4	1
31	NDUFA6	35	6	3	2	1
32	UQCRB	35	8	2	5	1
33	MRPS9	33	3	0	3	0
34	NDUFB2	33	6	1	5	0
35	NDUFB6	33	5	0	5	0
36	NDUFS2	33	3	1	2	0
37	ATP5B	32	5	2	3	0
38	ATP5L	32	6	2	3	1
39	MRPL39	32	2	0	2	0
40	NDUFB4	32	4	0	4	0
41	MRPS30	31	2	0	2	0
42	NDUFA1	31	6	1	5	0
43	NDUFB11	31	4	0	3	1
44	TUFM	31	0	0	0	0
45	MRPL12	30	2	1	1	0
46	MRPL17	30	3	1	2	0
47	MRPL19	30	5	0	5	0

(Continued)

Table 4. (Continued)

S.No.	Protein	Neighbours	DEGs	Up DEG	Down DEG	mixed DEGs
48	MRPL27	30	2	1	1	0
49	MRPL40	30	2	0	2	0
50	SDHA	30	2	0	2	0

The table shows the number of first neighbours, the number of DEGs, and number of up/down-regulated DEGs among the first neighbours.

<https://doi.org/10.1371/journal.pone.0224632.t004>

We chose four representative hubs from the top right-side rectangle to draw their subnetworks with immediate connecting proteins (points marked red in the scatter plot, Fig 3). One of these hubs, UQCR10, which is a subunit of the respiratory chain complex III, is connected to 50 proteins, including two up- and six down-regulated DEGs (Table 5). The DEGs include the up-regulated complex 1 subunit NDUFB7 and complex III subunit UQCR11; the down-

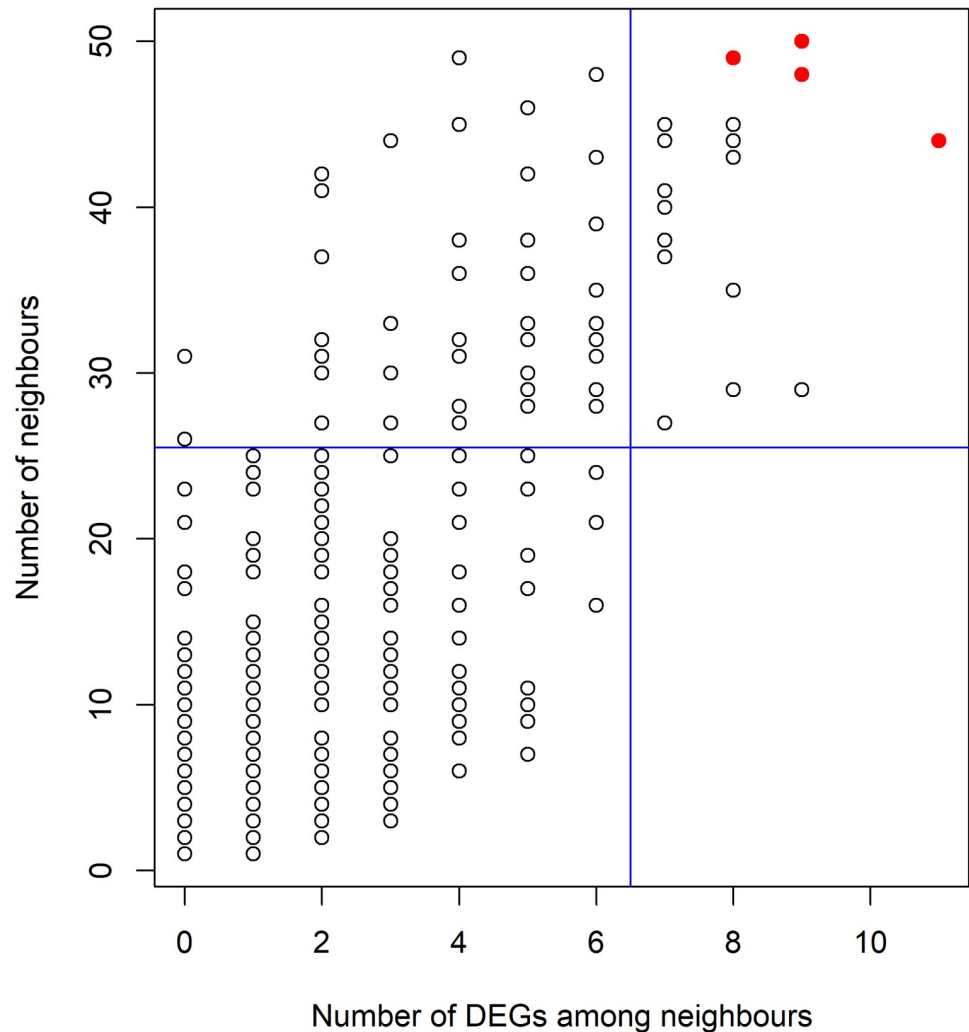


Fig 3. The scatterplot showing the relation between the number of neighbours and DEGs among them. The right top rectangle shows hub proteins with a high number of neighbours as well as DEGs among neighbours. The four circles represented in red colour correspond to NDUFS6, UQCR10, UQCRQ and NDUFV2.

<https://doi.org/10.1371/journal.pone.0224632.g003>

Table 5. The important hubs with a high number of neighbours and DEGs among them.

S.No.	Protein	Neighbours	DEGs	Up DEG	Down DEG	Mixed DEGs
1	NDUFS6	44	11	4	6	1
2	UQCR10	50	9	2	6	1
3	UQCRQ	48	9	3	5	1
4	ACLY	29	9	5	4	0
5	NDUFV2	49	8	0	7	1
6	NDUFA13	45	8	2	5	1
7	ATP5O	44	8	2	5	1
8	NDUFAB1	43	8	1	6	1
9	UQCRB	35	8	2	5	1
10	NDUFA12	29	8	2	5	1
11	NDUFB8	45	7	2	4	1
12	UQCRFS1	44	7	2	4	1
13	ATP5C1	41	7	1	5	1
14	NDUFB10	41	7	1	5	1
15	NDUFA9	40	7	2	4	1
16	COX5B	38	7	2	4	1
17	NDUFA2	37	7	2	5	0
18	ATP5H	27	7	3	2	2

<https://doi.org/10.1371/journal.pone.0224632.t005>

regulated complex IV subunit COX7A1, complex I subunits, NDUFA4, NDUFB4, NDUFB6 and NDUFB9, and complex III subunit UQCRFS1 (S14 Fig). Another hub, NDUFV2 is linked to 49 proteins, including eight DEGs, seven of which, namely NDUFA4, NDUFB4, NDUFB6, NDUFB9, NDUFS4, PITRM1 and UQCRFS1, were down-regulated and one gene was mixed-regulated (S15 Fig).

The third hub, NDUFS6 links to 11 DEGs: four of these were up-regulated and are part of complex III (UQCR11), complex I (NDUFB7), complex IV (COX15) and complex V (ATP5E); six were down-regulated, of which ECHDC2 is implicated in the lyase activity, and the rest (NDUFA4, NDUFB4, NDUFB6, NDUFB9 and NDUFS4) are complex 1 subunits (S16 Fig).

The hub protein UQCRQ links to nine neighbours, of which three were up-regulated (UQCR11, NDUFB7 and ATP5E); and five were down-regulated (NDUFA4, NDUFB4, NDUFB6, NDUFS4 and UQCRFS1) (S17 Fig).

Gene ontology (GO) and pathway enrichment of the mitochondrial DEGs

The GO and pathway analyses were performed for the mitochondrial DEGs that were selected in at least two datasets (83 genes), using the STRING database. The results illustrated their roles at different levels, including MF, BP and CC. A total of 14 MF, 63 BP and 16 CC GO terms, and 3 KEGG pathways were significantly enriched (FDR < 0.01). Several of these terms and pathways were shared by both the up- and down-regulated DEGs. Some of the significantly enriched BP and MF GO terms are shown in Fig 4. The detailed lists of all the GO terms and KEGG pathways could be found in S4 Table and Tables 6–8.

Among the BP terms, the processes pertaining to metabolism, mitochondrial membrane permeability, regulation of membrane potential, oxidative stress, mitochondrial transport and apoptotic processes were enriched with DEGs (Fig 4 and S4 Table). Similarly, among the MF terms, the functions related to the binding of coenzymes and cofactors were enormously

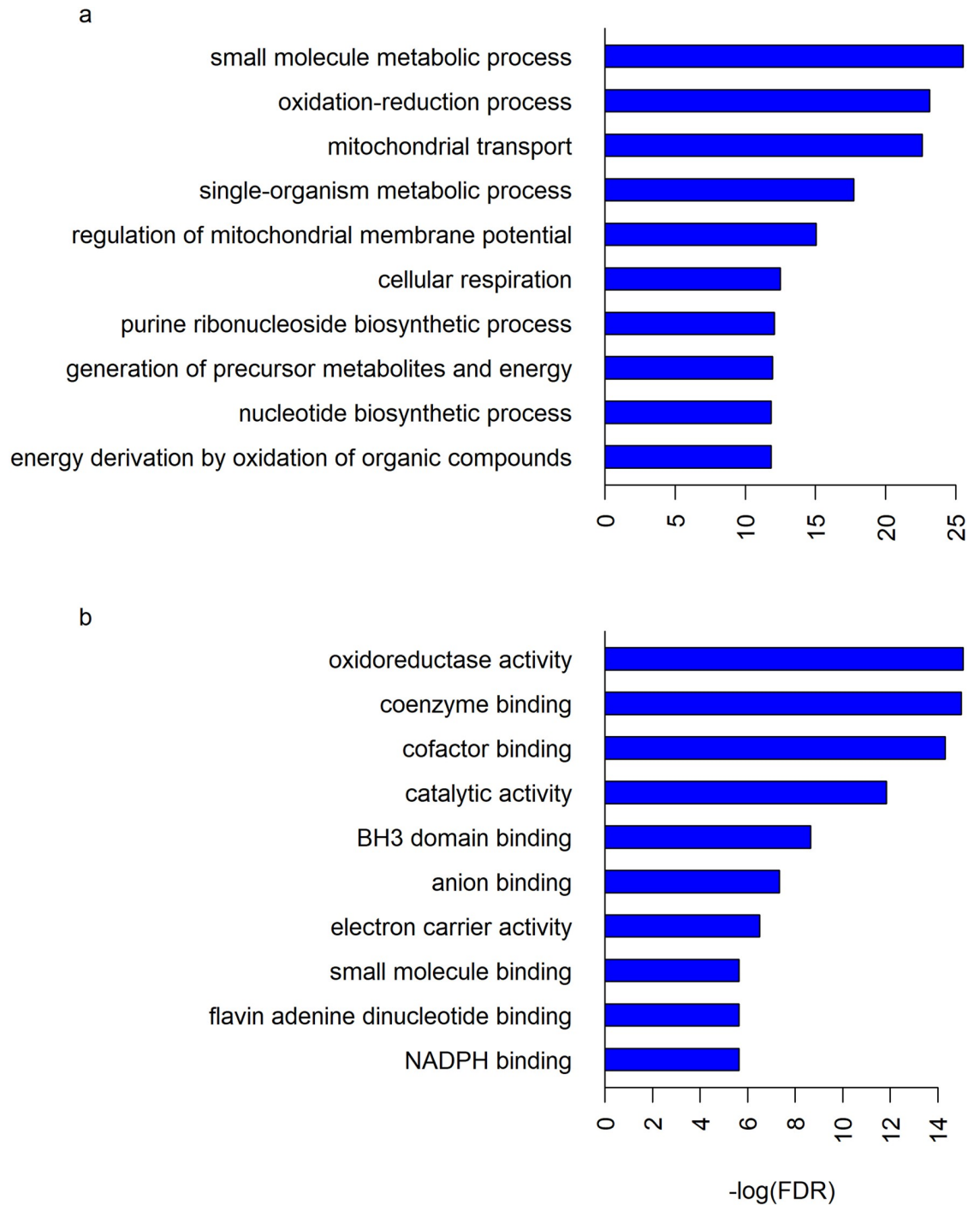


Fig 4. Some of the significantly enriched (a) BP and (b) MF GO terms. Each GO term was plotted against the negative logarithm of its false discovery rate (FDR) obtained from GO analysis using the STRING database, which uses hypergeometric test for determining significantly enriched GO terms [55–56].

<https://doi.org/10.1371/journal.pone.0224632.g004>

Table 6. The significantly enriched molecular functions (MF) of the RA synovial mitochondrial DEGs.

S.No.	Pathway ID	Pathway description	Observed gene count	False discovery rate
1	GO.0016491	oxidoreductase activity	18	2.85E-07
2	GO.0050662	coenzyme binding	11	3.06E-07
3	GO.0048037	cofactor binding	12	6.02E-07
4	GO.0003824	catalytic activity	44	7.19E-06
5	GO.0051434	BH3 domain binding	3	0.000176
6	GO.0043168	anion binding	27	0.000651
7	GO.0009055	electron carrier activity	6	0.00149
8	GO.0036094	small molecule binding	25	0.00356
9	GO.0050660	flavin adenine dinucleotide binding	5	0.00356
10	GO.0070402	NADPH binding	3	0.00356
11	GO.0000166	nucleotide binding	23	0.00471
12	GO.0046899	nucleoside triphosphate adenylate kinase activity	2	0.00471
13	GO.0022857	transmembrane transporter activity	13	0.0067
14	GO.0050661	NADP binding	4	0.00833333

<https://doi.org/10.1371/journal.pone.0224632.t006>

Table 7. The significantly enriched cellular components (CC) of the RA synovial mitochondrial DEGs.

S.No.	Pathway ID	Pathway description	Observed gene count	False discovery rate
1	GO.0005739	Mitochondrion	61	1.16E-47
2	GO.0044429	mitochondrial part	43	5.65E-35
3	GO.0005740	mitochondrial envelope	38	2.20E-32
4	GO.0031966	mitochondrial membrane	35	5.41E-29
5	GO.0031967	organelle envelope	39	6.11E-27
6	GO.0019866	organelle inner membrane	27	3.67E-21
7	GO.0005743	mitochondrial inner membrane	26	7.18E-21
8	GO.0005741	mitochondrial outer membrane	14	1.49E-13
9	GO.0005759	mitochondrial matrix	17	6.25E-12
10	GO.0031090	organelle membrane	39	2.37E-11
11	GO.0044444	cytoplasmic part	58	5.34E-10
12	GO.0005737	Cytoplasm	59	9.81E-05
13	GO.0044446	intracellular organelle part	49	0.000261
14	GO.0044455	mitochondrial membrane part	7	0.000336
15	GO.0043231	intracellular membrane-bounded organelle	58	0.000913
16	GO.0097136	Bcl-2 family protein complex	2	0.00794

<https://doi.org/10.1371/journal.pone.0224632.t007>

enriched with DEGs (Fig 4 and Table 6). Additionally, DEGs were enriched in many mitochondrial CC terms (Table 7).

Among the enriched KEGG pathways, ‘metabolic pathways’ (KEGG pathway ID: 1100) is highly enriched with 20 DEGs. Of the others, glycine, serine, threonine and glutathione metabolisms were affected (Table 8).

Table 8. The significantly enriched KEGG pathways of the RA synovial mitochondrial DEGs.

S.No.	Pathway ID	Pathway description	Observed gene count	False discovery rate
1	1100	Metabolic pathways	20	7.81E-06
2	260	Glycine, serine and threonine metabolism	5	7.21E-05
3	480	Glutathione metabolism	4	0.00444

<https://doi.org/10.1371/journal.pone.0224632.t008>

Disruption of OxPhos in the RA synovium

From the enriched MF items, it is understood that the oxidoreductase activity is getting affected in RA. This activity is associated with the OxPhos complexes of mitochondria. There are five complexes: complex I, II, III, IV and V. Electrons from NADH and FADH₂ pass through the first four complexes and eventually reduce O₂ to water at complex IV. Overall, the complexes have 97 subunits, 84 of which are encoded by nDNA. The created mitochondrial PPI network contains 81 of the 84 subunits. Totally, 11 of them were DEGs in one or two datasets (Table 9). The complex I DEGs, NDUFB4, NDUFB6, NDUFB9 and NDUFS4 were down-regulated. At least one gene each in complex III, complex IV and complex V was down or up-regulated. UQCRFS1 of complex III, COX6A1 and COX7A1 of complex IV, and ATP5G3 of complex V were down-regulated. The mitochondrial protein-coding genes of OxPhos were either missed or non-DEGs in the microarray studies. From these observations, it can be deduced that OxPhos is getting disrupted, perhaps impaired due to the decreased expression of some of the OxPhos genes in the RA synovium. This might be concerned with the escape of electrons from OxPhos, leading to the formation of ROS. Nevertheless, since 11 of the subunits are DEGs in either one or two datasets, it may be difficult to come to a concrete conclusion.

ROS detoxification and apoptosis in the RA synovium

The ROS generating NADPH oxidases (NOXs), such as NOX1, NOX2 and NOX3 were not DEGs, and NOX4 was down in two and up in one microarray datasets. This might be indicating that it is the mitochondria, and not these enzymes, that could be the primary source of ROS in RA. The detoxifiers of ROS, such as catalase (CAT), glutathione peroxidase 4 (GPX4) and superoxide dismutase 1 (SOD1) were down-regulated in one dataset, specifying impaired detoxification. Further, LAP3, which degrades glutathione, was overexpressed in five datasets. This gives a clue for the accumulation of mitochondrial ROS (mtROS), which might induce apoptosis in RA synoviocytes. In support of this, the pro-apoptotic BAX was up-regulated in two datasets. The executor of apoptosis, CASP8 was up in three. However, CASP8, in the presence of FLIP, is known to induce inflammation rather than apoptosis [45]. Further, H₂O₂ might trigger apoptosis by causing elevation of intracellular Ca²⁺ levels via a pathway that includes spleen tyrosine kinase (SYK), Bruton's tyrosine kinase (BTK), the B cell linker protein (BLNK) and phospholipase Cγ2 (PLCγ2) [74–75]. Interestingly, these four genes were up-

Table 9. The differential expression of the subunits of mitochondrial respiratory chain complexes and their maximum fold-changes.

S. No.	Gene	Number of synovial datasets with up-regulation	Number of synovial datasets with down-regulation	Mitochondrial respiratory chain complex	Max fold-change
1	NDUFB4	0	1	I	1.62 ↓
2	NDUFB6	0	1	I	1.7 ↓
3	NDUFB7	1	0	I	1.76 ↑
4	NDUFB9	0	1	I	1.76 ↓
5	NDUFS4	0	1	I	2.15 ↓
6	UQCRFS1	0	1	III	1.69 ↓
7	UQCR11	1	0	III	1.51 ↑
8	COX6A1	1	1	IV	1.63 ↑
9	COX7A1	0	2	IV	2.94 ↓
10	ATP5E	2	0	V	1.58 ↑
11	ATP5G3	0	1	V	1.73 ↓

The up and down arrows indicate up and down-regulation, respectively.

<https://doi.org/10.1371/journal.pone.0224632.t009>

regulated in at least three datasets. SYK, BTK, BLNK and PLC γ 2 were up-regulated in six, three, five and six datasets, respectively. But, Bcl-2-like 1 (BCL2L1) protein, which controls the production of ROS by regulating membrane potential, was mixed-regulated, making it difficult to conclude on its role. Further, the anti-apoptotic protein Bcl-2 (BCL2) was mixed-regulated. Surprisingly, the pro-apoptotic Bcl-2-like 13 (BCL2L13) was down in one dataset. Collectively, the results may suggest (i) generation of mtROS, (ii) impaired ROS detoxification and (iii) induction of mitochondrion-initiated intrinsic apoptosis in the RA synovium.

A model relating mtROS and inflammation in the RA synovium

Since NOXs are less expressed, mitochondria might be the primary generators of ROS in the RA synovium. A component of ROS, O $_2^{\cdot-}$ may interact with nitric oxide (NO), which is abundant in RA [76–81], resulting in the formation of ONOO $^-$. The molecule ONOO $^-$ is involved in the activation of the I κ B kinase (IKK) through a mechanism that depletes the-SH groups of glutathione [43]. Our analysis also indicated an increased degradation of glutathione, possibly by the enzyme LAP3. Active IKK degrades its substrate I κ B, resulting in the translocation of NF- κ B to the nucleus, where it induces the expression of inflammatory mediators, such as TNF, IL-1 β and iNOS. The enzyme iNOS catalyses the production of NO from arginine and hence might further potentiate the production of ONOO $^-$ (Fig 5). Furthermore, damaged mitochondria can release molecules, called the damage-associated molecular patterns (DAMPs), which contribute to inflammation [82]. Taken together, mitochondrial production of ROS and their involvement in NF- κ B activation, increased glutathione degradation, and DAMPs released from damaged mitochondria suggest that this cell organelle is associated with the induction and maintenance of inflammation in the RA synovium.

Discussion

Many researchers had created PPI networks for RA at the level of a cell. For instance, in order to identify key molecules, earlier we had created a PPI network for cytokine signalling in RA [83]. Similarly, few studies had identified highly connected regions, ego networks and key genes in PPI networks in RA and other diseases [84–86]. Another study used PPI for determining the efficacy of leflunomide and ligustrazine drugs in the treatment of RA [87]. In contrast, in this study, we created, for the first time, a PPI network that is specific to RA synovial mitochondria and identified hub proteins. This network was created using reliable interactions from seven databases and gene expression data from six open-source microarray datasets. The network has 665 genes, of which 131 are DEGs.

The GO analysis of DEGs has given enriched processes, functions, cell components and KEGG pathways. ‘Oxidoreductase activity’ is the highest enriched molecular function. In general, several metabolic mechanisms, including OxPhos and pathways related to nucleotide, amino acid and glutathione seem to be affected. The analysis also identified the enriched oxidative stress, electron carrier activity, membrane permeability and apoptosis-related GO terms with DEGs.

The analysis of six microarray datasets gave 208 mitochondrial DEGs. Among them, the up-regulation of IFI27, which is involved in cytokine-mediated apoptosis, is in agreement with other RA studies [88]. The enzyme PDK1 was up-regulated. It is involved in hypoxia- and oxidative stress-mediated apoptosis, and is known to induce Akt pathway in human mast cells—which are abundantly seen in the RA synovium [89]. This enzyme also induces cell invasion and secretion of IL-1 β and IL-6 in a ribosomal S6 kinase (RSK2)-dependent TNF pathway in FLS [90]. AKR1B10 was down-regulated in three datasets. There is evidence that hypoxia induces the down-regulation of this gene in RA and healthy FLS [91]. EFHD1, which is a

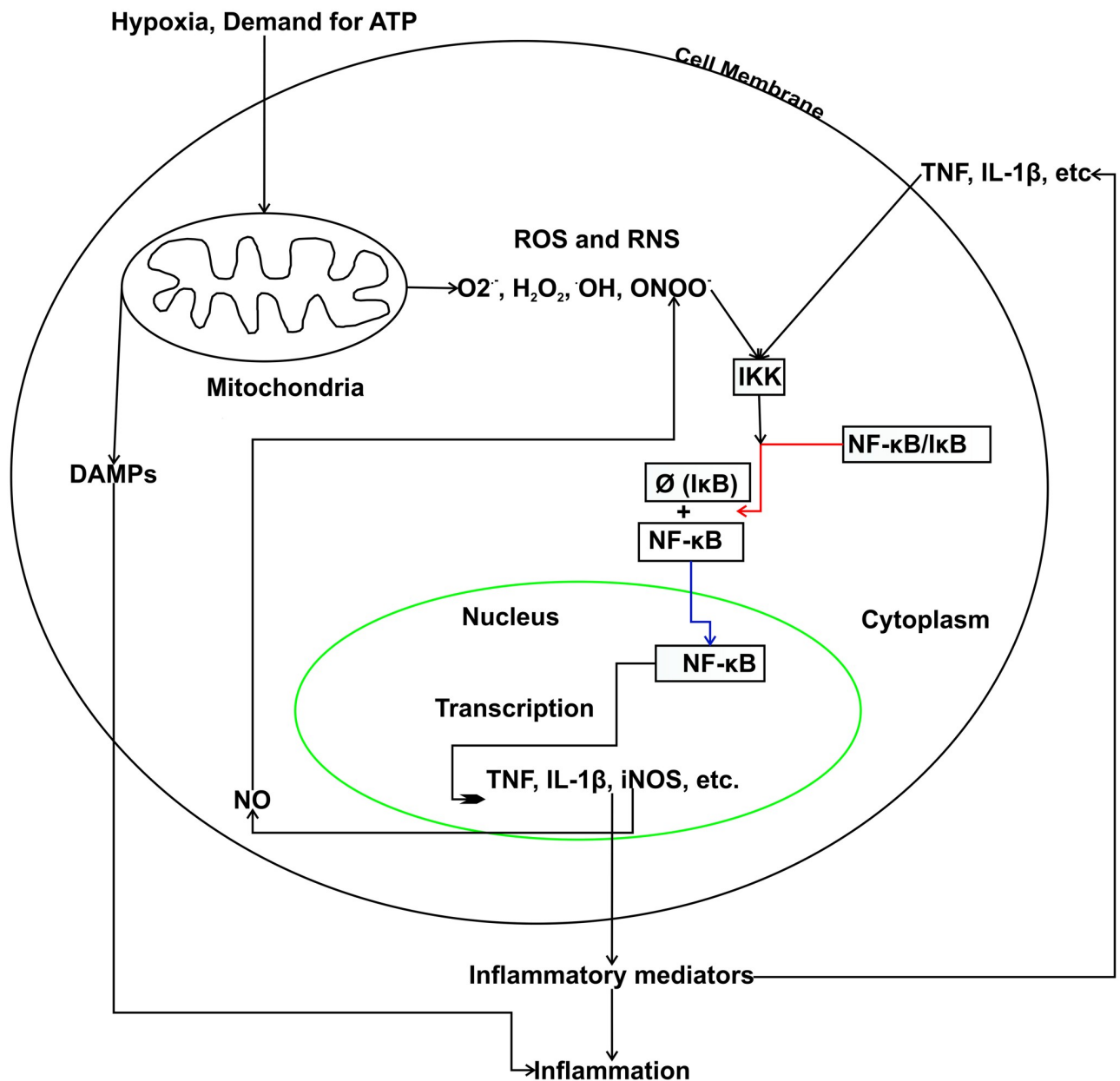


Fig 5. The proposed model for the relation between mitochondrial dysfunction and inflammation in RA. Hypoxia and demand for more ATP increase the production of mtROS and RNS, which activate the IKK enzyme that degrades IκB (degradation is represented with \emptyset). This results in the activation of transcription factor NF-κB that induces the expression of inflammatory mediators, such as tumour necrosis factor (TNF), interleukin-1 beta (IL-1β) and inducible nitric oxide synthase (iNOS). Further, the damage-associated molecular patterns (DAMPs) may also contribute to inflammation.

<https://doi.org/10.1371/journal.pone.0224632.g005>

calcium-binding protein and known to promote cell death, was down-regulated [92]. The enzyme ACOT7, which increases the concentration of free fatty acids (FFA) by hydrolysing the acyl-CoA thioester of long-chain fatty acids, such as palmitoyl-CoA, was up-regulated in five datasets. This enzyme could be implicated in the remodelling of membrane phospholipids [93]. UCP2 uncouples OxPhos pathway and has been identified a candidate risk gene for RA by a whole genome association study [94]. This protein, which gets activated by H_2O_2 and O_2^- , was up-regulated in the microarray data. The uncoupling of OxPhos by UCP2 leads to

the dissipation of mitochondrial membrane potential gradient. Moreover, FFAs produced by ACOT7 are likely to play a role in the uncoupling by increasing the production of ROS [95].

A high ratio of kynurenine/tryptophan, which was observed in sera of RA patients, is needed for the kynurenine pathway for its role in anti-inflammation [96–97]. In our analysis, since KMO, which catalyses the hydroxylation of kynurenine to 3-hydroxykynurenine, was up-regulated in five datasets; it may deplete the concentration of kynurenine thereby impairing its activity in controlling inflammation. Further, this might enhance the generation of free radicals [57]. The analysis also identified the disruption of OxPhos: 11 subunits of OxPhos complexes were DEGs, of which seven were exclusively down-regulated, clearly indicating the negative regulation of OxPhos. This may further be involved in ROS production. Collectively, these results suggest that free radicals, negative regulation of OxPhos, and metabolic processes are highly active in RA synovial mitochondria.

Increased demand for ATP production on the respiratory machinery, and NOX enzymes are usually involved in ROS generation. But, the down-regulation of NOXs provides a strong support of ROS production by mitochondria rather than by the enzymes in the RA synovium. The observed down-regulation of the detoxifiers of ROS, such as CAT, GPX4 and SOD1 is consistent with other RA studies [98–100]. Since there is no up-regulation of any of these enzymes in any of the six microarray datasets, the detoxification of free radicals might be impaired. Further, LAP3, which degrades glutathione and plays a crucial role in cartilage and bone erosion, was up-regulated [101]. Apart from this, CASP8, an apoptotic caspase and a risk gene for RA, was up-regulated. But, in RA FLS, it is known to induce the activation of pro-inflammatory NF- κ B and AP-1 transcription factors rather than apoptosis [45]. However, apoptosis may happen by a ROS-mediated increase in intracellular Ca^{2+} levels, preferably through the SYK, BTK, BLNK and PLC γ 2-mediated pathway. But it may nevertheless be insufficient to limit synovial hyperplasia. Thus, our results bring together enhanced oxidative stress and intrinsic apoptosis, with the up-regulation of processes involved in the generation of free radicals and with their impaired detoxification. These can be envisaged as a potential therapeutic strategy for RA. With regard to the network analysis, we show that UQCR10, MRPL4 and NDUFV2 are the three top hubs of the PPI network. UQCR10 belongs to the complex III, which is the middle segment of OxPhos, and is connected to 50 neighbours, of which nine were DEGs. This suggests a key role for this gene in the OxPhos pathway in RA synoviocytes. MRPL4, a part of the large 39S subunit of the mitochondrial ribosome, forms 49 PPI with neighbours. The complex I protein NDUFV2 is connected to 49 neighbours, including eight DEGs. Another complex I protein NDUFS6 has the maximum number of neighbour DEGs in the network. Since these proteins are the top hubs and have neighbour DEGs, it would be interesting to elucidate their roles in RA.

In this study, using publicly available microarray data, we discussed the roles of nDNA encoded proteins in RA mitochondrial dysfunction. Although the literature provides support to some of the inferences we made in the study, they need to be validated using experiments on cell lines or laboratory animals or in clinical studies. The expression levels of mtDNA encoded genes that were not probed by the microarray platforms could not be assessed in this study. Further, as the composition of cell types is different in both the healthy and RA synovial tissues, the changes in gene expression between them may be a manifestation of the respective cell types present in them.

Conclusions

In conclusion, our study maximises the use of PPI and microarray data for studying mitochondrial dysfunction in RA. Identifying a set of nDNA encoded mitochondrial proteins implicated

in the dysregulation of pathways and processes associated with this organelle in the RA synovium was the idea behind this study. Analysing microarray data for identifying DEGs and understanding their likely functions in synovial mitochondria is highly informative in this context. Using DEGs, we identified the processes pertaining to the generation of free radicals and their impaired detoxification. The study also reports the possible occurrence of the mitochondrion-mediated intrinsic apoptotic pathway in RA. We also, in particular, highlighted the roles of DEGs in the remodelling of membrane lipids, uncoupling electron transport and ATP synthesis, and amino acid and nucleotide metabolism in RA. We also proposed a model that links mitochondrial dysfunction to inflammation in RA by collating information from the literature. These insights suggest several new routes for research into the role of mitochondria in RA. Particularly, oxidative stress and intrinsic apoptotic pathways may become attractive candidates for new therapeutic interventions. However, our strategy herein was to develop a proof-of-principle method for studying mitochondrial dysfunction by integrating gene expression, PPI, gene ontology and network analysis. Even though literature search has provided the possible implications for the study findings in RA mitochondrial dysfunction, their additional validation in experimental settings is needed.

Supporting information

S1 File. File for visualising the network using the Cytoscape tool. The up- and down-regulated genes are highlighted in green and red colours respectively.

(XGMML)

S1 Fig. A Venn diagram showing the translocation of the mitochondrial network genes to different parts of mitochondria.

(TIF)

S2 Fig. Hierarchical clustering of RA and control samples based on the gene expression of selected DEGs (Table 2) in GSE7307.

(TIF)

S3 Fig. Hierarchical clustering of RA and control samples based on the gene expression of selected DEGs (Table 2) in GSE55235.

(TIF)

S4 Fig. Hierarchical clustering of RA and control samples based on the gene expression of selected DEGs (Table 2) in GSE55457.

(TIF)

S5 Fig. Hierarchical clustering of RA and control samples based on the gene expression of selected DEGs (Table 2) in GSE12021 (HGU133A).

(TIF)

S6 Fig. Hierarchical clustering of RA and control samples based on the gene expression of selected DEGs (Table 2) in GSE12021 (HGU133B).

(TIF)

S7 Fig. Hierarchical clustering of RA and control samples based on the gene expression of selected DEGs (Table 2) in GSE77298.

(TIF)

S8 Fig. Hierarchical clustering of RA and control samples based on the gene expression of selected DEGs (Table 2) in GSE12021 (HGU133A) after removing RA samples clustered

with control samples.

(TIF)

S9 Fig. Hierarchical clustering of RA and control samples based on the gene expression of selected DEGs (Table 2) in GSE12021 (HGU133B) after removing RA samples clustered with control samples.

(TIF)

S10 Fig. Hierarchical clustering of prednisone treated and control samples (whole blood) based on the gene expression of selected DEGs (Table 2) normalized across samples in GSE77344.

(TIFF)

S11 Fig. Hierarchical clustering of celecoxib treated and control samples (colorectal primary adenocarcinomas) based on the gene expression of selected DEGs (Table 2) normalized across samples in GSE11237.

(TIFF)

S12 Fig. Hierarchical clustering of pre and post methotrexate treatment samples (early RA synovial biopsy) based on the gene expression of selected DEGs (Table 2) normalized across samples in GSE45867.

(TIFF)

S13 Fig. The distribution of the number of all neighbours and DEG neighbours of all the proteins of the mitochondrial PPI network.

(TIF)

S14 Fig. The subnetwork of UQCR10.

(TIF)

S15 Fig. The subnetwork of NDUFV2.

(TIF)

S16 Fig. The subnetwork of NDUF6.

(TIF)

S17 Fig. The subnetwork of UQCRC.

(TIF)

S1 Table. The number of microarray datasets in which the mitochondrial PPI network genes were differentially expressed.

(XLS)

S2 Table. The number of microarray datasets in which, the MitoCarta genes, which are not part of the network, were differentially expressed.

(XLSX)

S3 Table. Number of neighbours for all mitochondrial PPI network proteins. The table shows the number of first neighbours, the number of DEGs and number of up/down regulated DEGs among the first neighbours.

(XLSX)

S4 Table. The significantly enriched biological processes (BP) of the RA synovial mitochondrial DEGs.

(XLS)

Acknowledgments

We thank the Institute of Bioinformatics and Applied Biotechnology (IBAB) for providing facilities and the environment for carrying out this research work.

Author Contributions

Conceptualization: Venugopal Panga, Srivatsan Raghunathan.

Formal analysis: Venugopal Panga, Ashwin Adrian Kallor, Arunima Nair, Shilpa Harshan, Srivatsan Raghunathan.

Investigation: Venugopal Panga, Ashwin Adrian Kallor, Arunima Nair, Shilpa Harshan, Srivatsan Raghunathan.

Methodology: Venugopal Panga, Ashwin Adrian Kallor, Arunima Nair, Srivatsan Raghunathan.

Project administration: Srivatsan Raghunathan.

Resources: Srivatsan Raghunathan.

Software: Venugopal Panga, Ashwin Adrian Kallor, Arunima Nair, Shilpa Harshan.

Supervision: Srivatsan Raghunathan.

Validation: Shilpa Harshan.

Visualization: Venugopal Panga, Shilpa Harshan.

Writing – original draft: Venugopal Panga.

Writing – review & editing: Shilpa Harshan, Srivatsan Raghunathan.

References

1. Fearon U, Canavan M, Biniecka M, Veale DJ. Hypoxia, mitochondrial dysfunction and synovial invasiveness in rheumatoid arthritis. *Nat Rev Rheumatol*. 2016; 12: 385–97. <https://doi.org/10.1038/nrrheum.2016.69> PMID: 27225300
2. Medina-Gomez G. Mitochondrial and endocrine function of adipose tissue. *Best Pract Res Clin Endocrinol Metab*. 2012; 26: 791–804. <https://doi.org/10.1016/j.beem.2012.06.002> PMID: 23168280
3. Pagano G, Castello G, Pallardó FV. Sjögren's syndrome-associated oxidative stress and mitochondrial dysfunction: prospects for chemoprevention trials. *Free Radic Res*. 2013; 47: 71–3. <https://doi.org/10.3109/10715762.2012.748904> PMID: 23153390
4. Quang J, Wu M, Huang C, Cao L, Li G. Overexpression of oxidored-nitro domain containing protein 1 inhibits human nasopharyngeal carcinoma and cervical cancer cell proliferation and induces apoptosis: Involvement of mitochondrial apoptotic pathways. *Oncol Rep*. 2013; 29: 79–86. <https://doi.org/10.3892/or.2012.2101> PMID: 23124592
5. Osellame LD, Blacker TS, Duchon MR. Cellular and molecular mechanisms of mitochondrial function. *Best Pract Res Clin Endocrinol Metab*. 2012; 26: 711–23. <https://doi.org/10.1016/j.beem.2012.05.003> PMID: 23168274
6. Legault JT, Strittmatter L, Tardif J, Sharma R, Tremblay-Vaillancourt V, Aubut C, et al. A metabolic signature of mitochondrial dysfunction revealed through a monogenic form of Leigh syndrome. *Cell Rep*. 2015; 13(5): 981–89. <https://doi.org/10.1016/j.celrep.2015.09.054> PMID: 26565911
7. Bick AG, Wakimoto H, Kamer KJ, Sancak Y, Goldberger O, Axelsson A, et al. Cardiovascular homeostasis dependence on MICU2, a regulatory subunit of the mitochondrial calcium uniporter. *Proc Natl Acad Sci*. 2017; 114(43): e9096–9104. <https://doi.org/10.1073/pnas.1711303114> PMID: 29073106
8. Lake NJ, Webb BD, Stroud DA, Richman TR, Ruzzenente B, Compton AG, et al. Biallelic mutations in MRPS34 lead to instability of the small mitoribosomal subunit and Leigh syndrome. *Am J Hum Genet*. 2017; 101(2): 239–54. <https://doi.org/10.1016/j.ajhg.2017.07.005> PMID: 28777931

9. Dai N, Zhao L, Wrighting D, Krämer D, Majithia A, Wang Y, et al. IGF2BP2/IMP2-deficient mice resist obesity through enhanced translation of Ucp1 mRNA and other mRNAs encoding mitochondrial proteins. *Cell Metab.* 2015; 21(4): 609–21. <https://doi.org/10.1016/j.cmet.2015.03.006> PMID: 25863250
10. Tucker EJ, Hershman SG, Kohrer C, Belcher-Timme CA, Patel J, Goldberger OA, et al. Mutations in MTFMT underlie a human disorder of formylation causing impaired mitochondrial translation. *Cell Metab.* 2011; 14(3): 428–34. <https://doi.org/10.1016/j.cmet.2011.07.010> PMID: 21907147
11. Fassone E, Duncan AJ, Taanman JW, Pagnamenta AT, Sadowski MI, Holand T, et al. FOXRED1, encoding an FAD-dependent oxidoreductase complex-I-specific molecular chaperone, is mutated in infantile-onset mitochondrial encephalopathy. *Hum Mol Genet.* 2010; 19(24): 4837–47. <https://doi.org/10.1093/hmg/ddq414> PMID: 20858599
12. Gohil VM, Nilsson R, Belcher-Timme CA, Luo B, Root DE, Mootha VK. Mitochondrial and nuclear genomic responses to loss of LRPPRC expression. *J Biol Chem.* 2010; 285(18): 13742–7. <https://doi.org/10.1074/jbc.M109.098400> PMID: 20220140
13. Kamer KJ, Mootha VK. MICU1 and MICU2 play nonredundant roles in the regulation of the mitochondrial calcium uniporter. *EMBO Rep.* 2014; 15(3): 299–07. <https://doi.org/10.1002/embr.201337946> PMID: 24503055
14. Sancak Y, Markhard AL, Kitami T, Kovács-Bogdán E, Kamer KJ, Udeshi ND, et al. EMRE is an essential component of the mitochondrial calcium uniporter complex. *Science.* 2013; 342(6164): 1379–82. <https://doi.org/10.1126/science.1242993> PMID: 24231807
15. Plovanich M, Bogorad RL, Sancak Y, Kamer KJ, Strittmatter L, Li AA, et al. MICU2, a paralog of MICU1, resides within the mitochondrial uniporter complex to regulate calcium handling. *Plos One.* 2013; 8(2): e55785. <https://doi.org/10.1371/journal.pone.0055785> PMID: 23409044
16. Calvo SE, Clauser KR, Mootha VK. MitoCarta2.0: an updated inventory of mammalian mitochondrial proteins. *Nucleic Acids Res.* 2016; 44: D1251–7. <https://doi.org/10.1093/nar/gkv1003> PMID: 26450961
17. McInnes IB, Schett G. Cytokines in the pathogenesis of rheumatoid arthritis. *Nat Rev Immunol.* 2007; 7(6): 429–42. <https://doi.org/10.1038/nri2094> PMID: 17525752
18. Moelants EA, Mortier A, Van Damme J, Proost P. Regulation of TNF-alpha with a focus on rheumatoid arthritis. *Immunol Cell Biol.* 2013; 91: 393–401. <https://doi.org/10.1038/icb.2013.15> PMID: 23628802
19. Smith MD. The normal synovium. *Open Rheumatol J.* 2011; 5: 100–06. <https://doi.org/10.2174/1874312901105010100> PMID: 22279508
20. Bromley M, Woolley DE. Histopathology of the rheumatoid lesion. Identification of cell types at sites of cartilage erosion. *Arthritis Rheum.* 1984; 27(8): 857–63. <https://doi.org/10.1002/art.1780270804> PMID: 6466394
21. Tak PP, Bresnihan B. The pathogenesis and prevention of joint damage in rheumatoid arthritis: advances from synovial biopsy and tissue analysis. *Arthritis Rheum.* 2000; 43(12): 2619–33. [https://doi.org/10.1002/1529-0131\(200012\)43:12<2619::AID-ANR1>3.0.CO;2-V](https://doi.org/10.1002/1529-0131(200012)43:12<2619::AID-ANR1>3.0.CO;2-V) PMID: 11145019
22. Ng CT, Biniiecka M, Kennedy A, McCormick J, FitzGerald O, Bresnihan B, et al. Synovial tissue hypoxia and inflammation in vivo. *Ann Rheum Dis.* 2010; 69(7): 1389–95. <https://doi.org/10.1136/ard.2009.119776> PMID: 20439288
23. Hildeman DA, Mitchell T, Kappler J, Marrack P. T cell apoptosis and reactive oxygen species. *J Clin Invest.* 2003; 111: 575–81. <https://doi.org/10.1172/JCI18007> PMID: 12618509
24. Kennedy A, Ng CT, Chang TC, Biniiecka M, O'Sullivan JN, Heffernan E, et al. Tumor necrosis factor blocking therapy alters joint inflammation and hypoxia. *Arthritis Rheum.* 2011; 63(4): 923–32. <https://doi.org/10.1002/art.30221> PMID: 21225682
25. Hitchon CA, El-Gabalawy HS. Oxidation in rheumatoid arthritis. *Arthritis Res Ther.* 2004; 6: 265–78. <https://doi.org/10.1186/ar1447> PMID: 15535839
26. Madamanchi NR, Runge MS. Mitochondrial dysfunction in atherosclerosis. *Circ Res.* 2007; 100: 460–73. <https://doi.org/10.1161/01.RES.0000258450.44413.96> PMID: 17332437
27. Kokoszka JE, Coskun P, Esposito LA, Wallace DC. Increased mitochondrial oxidative stress in the Sod2 (+/-) mouse results in the age-related decline of mitochondrial function culminating in increased apoptosis. *Proc Natl Acad Sci.* 2001; 98(5): 2278–83. <https://doi.org/10.1073/pnas.051627098> PMID: 11226230
28. Hajizadeh S, DeGroot J, TeKoppele JM, Tarkowski A, Collins LV. Extracellular mitochondrial DNA and oxidatively damaged DNA in synovial fluid of patients with rheumatoid arthritis. *Arthritis Res Ther.* 2003; 5: R234–40. <https://doi.org/10.1186/ar787> PMID: 12932286
29. Bashir S, Harris G, Denman MA, Blake DR, Winyard PG. Oxidative DNA damage and cellular sensitivity to oxidative stress in human autoimmune diseases. *Ann Rheum Dis.* 1993; 52: 659–66. <https://doi.org/10.1136/ard.52.9.659> PMID: 8239761

30. Lemarechal H, Allanore Y, Chenevier-Gobeaux C, Kahan A, Ekindjian OG, Borderie D, et al. Serum protein oxidation in patients with rheumatoid arthritis and effects of infliximab therapy. *Clin Chim Acta*. 2006; 372: 147–53. <https://doi.org/10.1016/j.cca.2006.04.002> PMID: 16716286
31. Dabbagh AJ, Trenam CW, Morris CJ, Blake DR. Iron in joint inflammation. *Ann Rheum Dis*. 1993; 52: 67–73. <https://doi.org/10.1136/ard.52.1.67> PMID: 8427520
32. Dai L, Lamb DJ, Leake DS, Kus ML, Jones HW, Morris CJ, et al. Evidence for oxidized low density lipoprotein in synovial fluid from rheumatoid arthritis patients. *Free Radic Res*. 2000; 32: 479–86. <https://doi.org/10.1080/1071576000300481> PMID: 10798713
33. Rowley D, Gutteridge JM, Blake D, Farr M, Halliwell B. Lipid peroxidation in rheumatoid arthritis: thio-barbituric acid-reactive material and catalytic iron salts in synovial fluid from rheumatoid patients. *Clin Sci (Lond)*. 1984; 66(6): 691–5.
34. Grootveld M, Henderson EB, Farrell A, Blake DR, Parkes HG, Haycock P. Oxidative damage to hyaluronate and glucose in synovial fluid during exercise of the inflamed rheumatoid joint. Detection of abnormal low-molecular-mass metabolites by proton-n.m.r. spectroscopy. *Biochem J*. 1991; 273: 459–67. <https://doi.org/10.1042/bj2730459> PMID: 1991041
35. Henrotin YE, Bruckner P, Pujol JPL. The role of reactive oxygen species in homeostasis and degradation of cartilage. *Osteoarthritis and Cartilage*. 2003; 11: 747–55. PMID: 13129694
36. Ushio-Fukai M, Tang Y, Fukai T, Dikalov SI, Ma Y, Fujimoto M, et al. Novel role of gp91^{phox}-containing NAD(P)H oxidase in vascular endothelial growth factor-induced signaling and angiogenesis. *Circ Res*. 2002; 91: 1160–67. <https://doi.org/10.1161/01.res.0000046227.65158.f8> PMID: 12480817
37. Cerhan JR, Saag KG, Merlino LA, Mikuls TR, Criswell LA. Antioxidant micronutrients and risk of rheumatoid arthritis in a cohort of older women. *Am J Epidemiol*. 2003; 157: 345–54.
38. Heliövaara M, Knekt P, Aho K, Aaran R-K, Alfthan G, Aromaa A. Serum antioxidants and risk of rheumatoid arthritis. *Ann Rheum Dis*. 1994; 53(1): 51–53. <https://doi.org/10.1136/ard.53.1.51> PMID: 8311556
39. Hagfors L, Leanderson P, Skoldstam L, Andersson J, Johansson G. Antioxidant intake, plasma antioxidants and oxidative stress in a randomized, controlled, parallel, Mediterranean dietary intervention study on patients with rheumatoid arthritis. *Nutr J*. 2003; 2: 5. <https://doi.org/10.1186/1475-2891-2-5> PMID: 12952549
40. Bae SC, Kim SJ, Sung MK. Inadequate antioxidant nutrient intake and altered plasma antioxidant status of rheumatoid arthritis patients. *J Am Coll Nutr*. 2003; 22(4): 311–5. <https://doi.org/10.1080/07315724.2003.10719309> PMID: 12897046
41. Paredes S, Girona J, Hurt-Camejo E, Vallvé JC, Olivé S, Heras M, et al. Antioxidant vitamins and lipid peroxidation in patients with rheumatoid arthritis: association with inflammatory markers. *J Rheumatol*. 2002; 29(11): 2271–7. PMID: 12415581
42. Mulherin DM, Thurnham DI, Situnayake RD. Glutathione reductase activity, riboflavin status, and disease activity in rheumatoid arthritis. *Ann Rheum Dis*. 1996; 55: 837–914. <https://doi.org/10.1136/ard.55.11.837> PMID: 8976642
43. Filippin LI, Vercelino R, Marroni NP, Xavier RM. Redox signalling and the inflammatory response in rheumatoid arthritis. *Clin Exp Immunol*. 2008; 152(3): 415–22. <https://doi.org/10.1111/j.1365-2249.2008.03634.x> PMID: 18422737
44. Li H, Wan A. Apoptosis of rheumatoid arthritis fibroblast-like synoviocytes: possible roles of nitric oxide and the thioredoxin 1. *Mediators Inflamm*. 2013; 2013(3): 953462.
45. Palao G, Santiago B, Galindo M, Rullas J, Alcamí J, Ramirez JC, et al. Fas activation of a proinflammatory program in rheumatoid synoviocytes and its regulation by FLIP and caspase 8 signaling. *Arthritis Rheum*. 2006; 54(5): 1473–81. <https://doi.org/10.1002/art.21768> PMID: 16646028
46. Chatr-Aryamontri A, Breitkreutz B-J, Oughtred R, Boucher L, Heinicke S, Chen D, et al. The BioGRID interaction database: 2015 update. *Nucleic Acids Res*. 2015; 43: D470–8. <https://doi.org/10.1093/nar/gku1204> PMID: 25428363
47. Orchard S, Ammari M, Aranda B, Breuza L, Briganti L, Broackes-Carter F, et al. The MintAct project—IntAct as a common curation platform for 11 molecular interaction databases. *Nucleic Acids Res*. 2014; 42: D358–63. <https://doi.org/10.1093/nar/gkt1115> PMID: 24234451
48. Chatr-Aryamontri A, Ceol A, Palazzi LM, Nardelli G, Schneider MV, Castagnoli L, et al. MINT: the molecular interaction database. *Nucleic Acids Res*. 2007; 35: D572–74. <https://doi.org/10.1093/nar/gkl950> PMID: 17135203
49. Szklarczyk D, Franceschini A, Wyder S, Forslund K, Heller D, Huerta-Cepas J, et al. STRING v10: protein-protein interaction networks, integrated over the tree of life. *Nucleic Acids Res*. 2015; 43(D1): D447–52.

50. Prasad TSK, Goel R, Kandasamy K, Keerthikumar S, Kumar S, Mathivanan S, et al. Human protein reference database—2009 update. *Nucleic Acids Res.* 2009; 37: D767–72. <https://doi.org/10.1093/nar/gkn892> PMID: 18988627
51. Salwinski L, Miller CS, Smith AJ, Pettit FK, Bowie JU, Eisenberg D. The database of interacting proteins: 2004 update. *Nucleic Acids Res.* 2004; 32: D449–51. <https://doi.org/10.1093/nar/gkh086> PMID: 14681454
52. Bossi A, Lehner B. Tissue specificity and the human protein interaction network. *Mol Syst Biol.* 2009; 5: 260. <https://doi.org/10.1038/msb.2009.17> PMID: 19357639
53. Huber R, Hummert C, Gausmann U, Pohlers D, Koczan D, Guthke R, et al. Identification of intra-group, inter-individual, and gene-specific variances in mRNA expression profiles in the rheumatoid arthritis synovial membrane. *Arthritis Res Ther.* 2008; 10(14): R98.
54. Woetzel D, Huber R, Kupfer P, Pohlers D, Pfaff M, Driesch D, et al. Identification of rheumatoid arthritis and osteoarthritis patients by transcriptome-based rule set generation. *Arthritis Res Ther.* 2014; 16: R84. <https://doi.org/10.1186/ar4526> PMID: 24690414
55. Franceschini A, Szklarczyk D, Frankild S, Kuhn M, Simonovic M, Roth A, et al. STRING v9.1: protein-protein interaction networks, with increased coverage and integration. *Nucleic Acids Res.* 2013; 41: D808–15. <https://doi.org/10.1093/nar/gks1094> PMID: 23203871
56. Rivals I, Personnaz L, Taing L, Marie-Claude P. Enrichment or depletion of a GO category within a class of genes: which test? *Bioinformatics.* 2007; 23(4): 401–07. <https://doi.org/10.1093/bioinformatics/btl633> PMID: 17182697
57. Dantzer R, O'Connor JC, Lawson MA, Kelley KW. Inflammation-associated depression: from serotonin to kynurenine. *Psychoneuroendocrinology.* 2011; 36(3): 426–36. <https://doi.org/10.1016/j.psyneuen.2010.09.012> PMID: 21041030
58. Kaur H, Ganguli D, Bachhawat AK. Glutathione degradation by the alternative pathway (DUG pathway) in *Saccharomyces cerevisiae* is initiated by (Dug2p-Dug3p)₂ complex, a novel glutamine amidotransferase (GATase) enzyme acting on glutathione. *J Biol Chem.* 2012; 287(12): 8920–31. <https://doi.org/10.1074/jbc.M111.327411> PMID: 22277648
59. Kim JW, Tchernyshyov I, Semenza GL, Dang CV. HIF-1-mediated expression of pyruvate dehydrogenase kinase: A metabolic switch required for cellular adaptation to hypoxia. *Cell Metab.* 2006; 3(3): 177–85. <https://doi.org/10.1016/j.cmet.2006.02.002> PMID: 16517405
60. Rosebeck S, Leaman DW. Mitochondrial localization and pro-apoptotic effects of the interferon-inducible protein ISG12a. *Apoptosis.* 2008; 13(4): 562–72. <https://doi.org/10.1007/s10495-008-0190-0> PMID: 18330707
61. Arsenijevic D, Onuma H, Pecqueur C, Raimbault S, Manning BS, Miroux B, et al. Disruption of the uncoupling protein-2 gene in mice reveals a role in immunity and reactive oxygen species production. *Nat Genet.* 2000; 26(4): 435–9. <https://doi.org/10.1038/82565> PMID: 11101840
62. Jin DY, Chae HZ, Rhee SG, Jeang KT. Regulatory role for a novel human thioredoxin peroxidase in NF-kappaB activation. *J Biol Chem.* 1997; 272(49): 30952–61. <https://doi.org/10.1074/jbc.272.49.30952> PMID: 9388242
63. Wang X, Wang L, Wang X, Sun F, Wang CC. Structural insights into the peroxidase activity and inactivation of human peroxiredoxin 4. *Biochem J.* 2012; 441(1): 113–8. <https://doi.org/10.1042/BJ20110380> PMID: 21916849
64. Hartmann B, Wai T, Hu H, MacVicar T, Musante L, Fischer-Zirnsak B, et al. Homozygous YME1L1 mutation causes mitochondrialopathy with optic atrophy and mitochondrial network fragmentation. *Elife.* 2016; 5:e16078. <https://doi.org/10.7554/eLife.16078> PMID: 27495975
65. Stiburek L, Cesnekova J, Kostkova O, Fornuskova D, Vinsova K, Wenchich L, et al. YME1L controls the accumulation of respiratory chain subunits and is required for apoptotic resistance, cristae morphogenesis, and cell proliferation. *Mol Biol Cell.* 2012; 23(6): 1010–23. <https://doi.org/10.1091/mbc.E11-08-0674> PMID: 22262461
66. Vishnivetskaya GB, Skriskaya JA, Seif I, Popova NK. Effect of MAO A deficiency on different kinds of aggression and social investigation in mice. *Aggress Behav.* 2007; 33(1): 1–6. <https://doi.org/10.1002/ab.20161> PMID: 17441000
67. Brunner HG, Nelen M, Breakefield XO, Ropers HH, van Oost BA. Abnormal behavior associated with a point mutation in the structural gene for monoamine oxidase A. *Science.* 1993; 262(5133): 578–80. <https://doi.org/10.1126/science.8211186> PMID: 8211186
68. Gupta V, Khan AA, Sasi BK, Mahapatra NR. Molecular mechanism of monoamine oxidase A gene regulation under inflammation and ischemia-like conditions: key roles of the transcription factors GATA2, Sp1 and TBP. *J Neurochem.* 2015; 134(1): 21–38. <https://doi.org/10.1111/jnc.13099> PMID: 25810277

69. Okada Y, Wu D, Trynka G, Raj T, Terao C, Ikan K, et al. Genetics of rheumatoid arthritis contributes to biology and drug discovery. *Nature*. 2014; 506: 376–81. <https://doi.org/10.1038/nature12873> PMID: 24390342
70. Shannon CP, Balshaw R, Chen V, Hollander Z, Toma M, McManus BM, et al. Enumerateblood—an R Package to Estimate the Cellular Composition of Whole Blood from Affymetrix Gene ST Gene Expression Profiles. *BMC Genomics*. 2017; 18: 43. <https://doi.org/10.1186/s12864-016-3460-1> PMID: 28061752
71. Auman JT, Church R, Lee SY, Watson MA, Fleshman JW, McLeod HL. Celecoxib Pre-Treatment in Human Colorectal Adenocarcinoma Patients Is Associated with Gene Expression Alterations Suggestive of Diminished Cellular Proliferation. *Eur J Cancer*. 2008; 44(12): 1754–60. <https://doi.org/10.1016/j.ejca.2008.05.010> PMID: 18653328
72. Ducreux J, Durez P, Galant C, Nzeusseu Toukap A, Van den Eynde B, Houssiau FA, et al. Global Molecular Effects of Tocilizumab Therapy in Rheumatoid Arthritis Synovium. *Arthritis Rheumatol*. 2014; 66(1): 15–23. <https://doi.org/10.1002/art.38202> PMID: 24449571
73. Barabási A-L, Gulbahce N, Loscalzo J. Network medicine: a network-based approach to human disease. *Nat Rev Genet*. 2011; 12: 56–58. <https://doi.org/10.1038/nrg2918> PMID: 21164525
74. Qin S, Chock PB. Bruton's tyrosine kinase is essential for hydrogen peroxide-induced calcium signaling. *Biochemistry*. 2001; 40(27): 8085–91. <https://doi.org/10.1021/bi0100788> PMID: 11434777
75. Olofsson MH, Havelka AM, Brnjic S, Shoshan MC, Linder S. Charting calcium-regulated apoptosis pathways using chemical biology: role of calmodulin kinase II. *BMC Chem Biol*. 2008; 8:2. <https://doi.org/10.1186/1472-6769-8-2> PMID: 18673549
76. Jang D, Murrell GAC. Nitric oxide in arthritis. *Free Radic Biol Med*. 1998; 24(9): 1511–9. [https://doi.org/10.1016/s0891-5849\(97\)00459-0](https://doi.org/10.1016/s0891-5849(97)00459-0) PMID: 9641270
77. van't Hof RJ, Hocking L, Wright PK, Ralston SH. Nitric oxide is a mediator of apoptosis in the rheumatoid joint. *Rheumatology*. 2000; 39: 1004–8. <https://doi.org/10.1093/rheumatology/39.9.1004> PMID: 10986306
78. Sakurai H, Kohsaka H, Liu MF, Higashiyama H, Hirata Y, Kanno K, et al. Nitric oxide production and inducible nitric oxide synthase expression in inflammatory arthritides. *J Clin Invest*. 1995; 96(5): 2357–63. <https://doi.org/10.1172/JCI118292> PMID: 7593623
79. Dey P, Panga V, Raghunathan S. A cytokine signaling network for the regulation of inducible nitric oxide synthase expression in rheumatoid arthritis. *Plos One*. 2016; 11(9): e0161306. <https://doi.org/10.1371/journal.pone.0161306> PMID: 27626941
80. Bauerová K, Bezek Š. Role of reactive oxygen and nitrogen species in etiopathogenesis of rheumatoid arthritis. *Gen Physiol Biophys*. 1999; 18: 15–20.
81. Phillips DC, Irundika Dias HK, Kitas GD, Griffiths HR. Aberrant reactive oxygen and nitrogen species generation in rheumatoid arthritis (RA): causes and consequences for immune function, cell survival, and therapeutic intervention. *Antioxid Redox Signal*. 2010; 12(6): 743–85. <https://doi.org/10.1089/ars.2009.2607> PMID: 19686039
82. Nakahira K, Hisata S, Choi AMK. The roles of mitochondrial damage-associated molecular patterns in diseases. *Antioxid Redox Signal*. 2015; 23: 1329–50. <https://doi.org/10.1089/ars.2015.6407> PMID: 26067258
83. Panga V, Raghunathan S. A cytokine protein-protein interaction network for identifying key molecules in rheumatoid arthritis. *Plos One*. 2018; 13(6): e0199530. <https://doi.org/10.1371/journal.pone.0199530> PMID: 29928007
84. Zhu N, Hou J, Wu Y, Li G, Liu J, Ma G, et al. Identification of key genes in rheumatoid arthritis and osteoarthritis based on bioinformatics analysis. *Medicine*. 2018; 97(22): e10997. <https://doi.org/10.1097/MD.00000000000010997> PMID: 29851858
85. Zhou WZ, Miao LG, Yuan H. Identification of significant ego networks and pathways in rheumatoid arthritis. *J Can Res Ther*. 2018; 14: 1024–8.
86. Sun Z, Wang W, Yu D, Mao Y. Differentially expressed genes between systemic sclerosis and rheumatoid arthritis. *Hereditas*. 2019; 156: 17. <https://doi.org/10.1186/s41065-019-0091-y> PMID: 31178673
87. Zhang C, Guan D, Jiang M, Liang C, Li L, Zhao N, et al. Efficacy of leflunomide combined with ligustrazine in the treatment of rheumatoid arthritis: prediction with network pharmacology and validation in a clinical trial. *Chin Med*. 2019; 14: 26. <https://doi.org/10.1186/s13020-019-0247-8> PMID: 31388350
88. Toro-Domínguez D, Carmona-Sáez P, Alarcón-Riquelme ME. Shared signatures between rheumatoid arthritis, systemic lupus erythematosus and Sjögren's syndrome uncovered through gene expression meta-analysis. *Arthritis Res Ther*. 2014; 16: 489. <https://doi.org/10.1186/s13075-014-0489-x> PMID: 25466291

89. Sawamukai N, Saito K, Yamaoka K, Nakayamada S, Ra C, Tanaka Y. Leflunomide inhibits PDK1/Akt pathway and induces apoptosis of human mast cells. *J Immunol*. 2007; 179(10): 6479–84. <https://doi.org/10.4049/jimmunol.179.10.6479> PMID: 17982036
90. Sun C, Sun Y, Jiang D, Bao G, Zhu X, Xu D, et al. PDK1 promotes the inflammatory progress of fibroblast-like synoviocytes by phosphorylating RSK2. *Cell Immunol*. 2017; 315: 27–33. <https://doi.org/10.1016/j.cellimm.2016.10.007> PMID: 28314444
91. Del Rey MJ, Izquierdo E, Usategui A, Gonzalo E, Blanco FJ, Acquadro F, et al. The transcriptional response of normal and rheumatoid arthritis synovial fibroblasts to hypoxia. *Arthritis Rheum*. 2010; 62(12): 3584–94. <https://doi.org/10.1002/art.27750> PMID: 20848564
92. Tominaga M, Kurihara H, Honda S, Amakawa G, Sakai T, Tomooka Y. Molecular characterization of mitocalcin, a novel mitochondrial Ca²⁺-binding protein with EF-hand and coiled-coil domains. *J Neurochem*. 2006; 96(1): 292–304. <https://doi.org/10.1111/j.1471-4159.2005.03554.x> PMID: 16336229
93. Wall VZ, Barnhart S, Kramer F, Kanter JE, Vivekanandan-Giri A, Pennathur S, et al. Inflammatory stimuli induce acyl-CoA thioesterase 7 and remodeling of phospholipids containing unsaturated long (\geq C20)-acyl chains in macrophages. *J Lipid Res*. 2017; 58: 1174–85. <https://doi.org/10.1194/jlr.M076489> PMID: 28416579
94. Tamiya G, Shinya M, Imanishi T, Ikuta T, Makino S, Okamoto K, et al. Whole genome association study of rheumatoid arthritis using 27039 microsatellites. *Hum Mol Genet*. 2005; 14(16): 2305–21. <https://doi.org/10.1093/hmg/ddi234> PMID: 16000323
95. Fariss MW, Chan CB, Patel M, Van Houten B, Orrenius S. Role of mitochondria in toxic oxidative stress. *Mol Interv*. 2005; 5(2): 94–111. <https://doi.org/10.1124/mi.5.2.7> PMID: 15821158
96. Schroecksnadel K, Kaser S, Ledochowski M, Neurauder G, Mur E, Herold M, et al. Increased degradation of tryptophan in blood of patients with rheumatoid arthritis. *J Rheumatol*. 2003; 30: 1935–9. PMID: 12966593
97. Kolodziej L. An exploratory study of the interplay between decreased concentration of tryptophan, accumulation of kynurenines, and inflammatory arthritis. *IUBMB Life*. 2012; 64(12): 983–87. <https://doi.org/10.1002/iub.1092> PMID: 23124849
98. Taysi S, Polat F, Gul M, Sari RA, Bakan E. Lipid peroxidation, some extracellular antioxidants, and antioxidant enzymes in serum of patients with rheumatoid arthritis. *Rheumatol Int*. 2002; 21(5): 200–4. <https://doi.org/10.1007/s00296-001-0163-x> PMID: 11958437
99. Marklund SL, Bjelle A, Elmqvist LG. Superoxide dismutase isoenzymes of the synovial fluid in rheumatoid arthritis and in reactive arthritides. *Ann Rheum Dis*. 1986; 45: 847–51. <https://doi.org/10.1136/ard.45.10.847> PMID: 3789819
100. Ozturk HS, Cimen MY, Cimen OB, Kacmaz M, Durak I. Oxidant/antioxidant status of plasma samples from patients with rheumatoid arthritis. *Rheumatol Int*. 1999; 19: 35–37. <https://doi.org/10.1007/s002960050097> PMID: 10651080
101. Vainio U. Leucineaminopeptidase in rheumatoid arthritis. *Ann Rheum Dis*. 1970; 29: 434.